Atmospheric
Chemistry
and Physics

Analysis of the potential of near-ground measurements of CO_2 and CH_4 in London, UK, for the monitoring of city-scale emissions using an atmospheric transport model

Alex Boon[1], Grégoire Broquet[2], Deborah J. Clifford[1], Frédéric Chevallier[2], David M. Butterfield[3], Isabelle Pison[2], Michel Ramonet[2], Jean-Daniel Paris[2], and Philippe Ciais[2]

[1]Department of Meteorology, University of Reading, Reading, Berkshire RG6 6BB, UK
[2]Laboratoire des Sciences du Climat et de l'Environnement, CEA-CNRS-UVSQ, UMR8212, IPSL, Gif-sur-Yvette, France
[3]National Physical Laboratory, Teddington, Middlesex TW11 0LW, UK

Correspondence to: Grégoire Broquet (gregoire.broquet@lsce.ipsl.fr)

Abstract. Carbon dioxide (CO_2) and methane (CH_4) mole fractions were measured at four near-ground sites located in and around London during the summer of 2012 with a view to investigating the potential of assimilating such measurements in an atmospheric inversion system for the monitoring of the CO_2 and CH_4 emissions in the London area. These data were analysed and compared with simulations using a modelling framework suited to building an inversion system: a 2 km horizontal resolution south of England configuration of the transport model CHIMERE driven by European Centre for Medium-Range Weather Forecasts (ECMWF) meteorological forcing, coupled to a 1 km horizontal resolution emission inventory (the UK National Atmospheric Emission Inventory). First comparisons reveal that local sources, which cannot be represented in the model at a 2 km resolution, have a large impact on measurements. We evaluate methods to filter out the impact of some of the other critical sources of discrepancies between the measurements and the model simulation except that of the errors in the emission inventory, which we attempt to isolate. Such a separation of the impact of errors in the emission inventory should make it easier to identify the corrections that should be applied to the inventory. Analysis is supported by observations from meteorological sites around the city and a 3-week period of atmospheric mixing layer height estimations from lidar measurements. The difficulties of modelling the mixing layer depth and thus CO_2 and CH_4 concentrations during the night, morning and late afternoon lead to focusing on the afternoon period for

all further analyses. The discrepancies between observations and model simulations are high for both CO_2 and CH_4 (i.e. their root mean square (RMS) is between 8 and 12 parts per million (ppm) for CO_2 and between 30 and 55 parts per billion (ppb) for CH_4 at a given site). By analysing the gradients between the urban sites and a suburban or rural reference site, we are able to decrease the impact of uncertainties in the fluxes and transport outside the London area and in the model domain boundary conditions. We are thus able to better focus attention on the signature of London urban CO_2 and CH_4 emissions in the atmospheric CO_2 and CH_4 concentrations. This considerably improves the statistical agreement between the model and observations for CO_2 (with model–data RMS discrepancies that are between 3 and 7 ppm) and to a lesser degree for CH_4 (with model–data RMS discrepancies that are between 29 and 38 ppb). Between one of the urban sites and either the rural or suburban reference site, selecting the gradients during periods wherein the reference site is upwind of the urban site further decreases the statistics of the discrepancies in general, though not systematically. In a further attempt to focus on the signature of the city anthropogenic emission in the mole fraction measurements, we use a theoretical ratio of gradients of carbon monoxide (CO) to gradients of CO_2 from fossil fuel emissions in the London area to diagnose observation-based fossil fuel CO_2 gradients, and compare them with the fossil fuel CO_2 gradients simulated with CHIMERE. This estimate increases the consistency between the model and the measurements when

considering only one of the two urban sites, even though the two sites are relatively close to each other within the city. While this study evaluates and highlights the merit of different approaches for increasing the consistency between the mesoscale model and the near-ground data, and while it manages to decrease the random component of the analysed model–data discrepancies to an extent that should not be prohibitive to extracting the signal from the London urban emissions, large biases, the sign of which depends on the measurement sites, remain in the final model–data discrepancies. Such biases are likely related to local emissions to which the urban near-ground sites are highly sensitive. This questions our current ability to exploit urban near-ground data for the atmospheric inversion of city emissions based on models at spatial resolution coarser than 2 km. Several measurement and modelling concepts are discussed to overcome this challenge.

1   Introduction

As major greenhouse gas (GHG) emitters, cities have an important part to play in national GHG emission reporting. Over half of the world's population now live in cities, and the UN estimates that the urban population will almost double from 3.4 to 6.3 billion by 2050 (United Nations, 2012). In the face of this continued urban population increase, cities can expect increased anthropogenic emissions unless measures are taken to reduce the impact of city life on the atmosphere. The majority of anthropogenic carbon dioxide (CO_2) is released in the combustion of fossil fuels for heating, electricity and transport, the latter of which is particularly important in the urban environment. The major sources of methane (CH_4) in city environments are leakage from natural gas infrastructure, landfill sites, wastewater treatment and transport emissions (Lowry et al., 2001; Nakagawa et al., 2005; Townsend-Small et al., 2012).

International agreements to limit GHG emissions make use of countries' self-reporting of emissions using emission inventories. These inventories are based upon activity data and corresponding emission factors and uncertainties can be substantial, particularly at the city scale. Ciais et al. (2010a) showed uncertainties of 19 % of the mean emissions at country scale in the 25 EU member states and up to 60 % at scales less than 200 km. Currently there is no legal obligation for individual cities to report their emissions; however, as environmental awareness increases and actions are taken to reduce urban GHG emissions, monitoring of city emissions to evaluate the success of emissions reduction schemes becomes an important consideration.

Quantifying GHG emissions from cities using an atmospheric inversion approach (i.e. based on gas mole fraction measurements, atmospheric transport modelling and statistical inference) is a relatively new scientific endeavour (Levin

et al., 2011; McKain et al., 2012; Kort et al., 2013; Bréon et al., 2015; Henne et al., 2016; Staufer et al., 2016). Instruments to measure urban GHG concentrations have been placed on tall masts or towers (at more than 50 m above the ground level, m a.g.l.) or at near-ground (at less than 20 m a.g.l.) heights (McKain et al., 2012; Lac et al., 2013; Bréon et al., 2015) with a preference generally given to higher-level measurement sites as these are expected to reduce variability due to local sources (Ciais et al., 2010b). The city-scale inversion studies have mainly focused on the monitoring of CO_2 city emissions. However, McKain et al. (2015) have shown the potential of the city-scale inversion approach to reduce uncertainties in CH_4 city emissions inventories, which can be substantial in cities, such as Boston (Massachusetts), where the gas distribution network has a high leakage level.

Near-ground sites are cheaper and easier to install and maintain than tall towers. There are far more choices of location for the placing of instrumentation near ground than on tall towers, even within a city. The development of cheaper instruments could enable the deployment of networks with numerous sites and this is likely to require placement of at least some sites on near-ground locations. If near-ground sites can be used effectively they could be highly complementary to the developing GHG observation networks. For their inversions of the Paris emissions, Bréon et al. (2015) and Staufer et al. (2016) used near-ground measurements taken in the suburban area of Paris but not in the city centre. They indicated that the capability of exploiting urban measurements would strongly improve the monitoring of the city emissions. Kort et al. (2013) evaluated (through observing system simulation experiments, which are a common practice in the data assimilation community, as detailed by Masutani et al., 2010) different configurations of surface station networks for monitoring emissions from Los Angeles, and concluded that robust monitoring of megacities requires multiple in-city surface sites (numbering at least eight stations for Los Angeles). McKain et al. (2012) employed near-ground sites in Salt Lake City, an urban area that is relatively small and topographically confined. They concluded that surface stations could be used to detect changes in GHG emissions at the monthly scale, but not to derive estimates of the absolute emissions because of the inability of current models to simulate small scale atmospheric processes.

Our study feeds such an investigation of the potential of city atmospheric inversion frameworks using continuous measurements at near-ground stations, including measurements within the urban area. We focus our attention on the megacity of London, UK. Previous studies of the GHG fluxes in London by the atmospheric community have largely focused on direct measurements of local fluxes using the eddy covariance technique, and on high-resolution transport modelling to identify the emission (spatial) footprint associated with these measurements (Helfter et al., 2011; Kotthaus and Grimmond, 2012; Ward et al., 2015). These local eddy co-

variance measurements in London have been used to derive estimates of the fluxes for specific boroughs or administrative areas (Helfter et al., 2011) and to compare the typical fluxes for different types of land use (Ward et al., 2015).

The atmospheric inversion approach, which is based on different estimation concepts and modelling scales to those of eddy covariance methods, has the potential to provide estimates of the emissions for a far larger portion of the city, and ideally for the city as a whole. Rigby et al. (2008) compared CO$_2$ concentration measurements from a central London site (Queen's Tower, Imperial College) with near-ground measurements at a more rural location (Royal Holloway University of London) upstream of the city in the prevailing wind direction. They thus characterised the CO$_2$ mole fraction enhancement as a result of the CO$_2$ emissions from anthropogenic sources in the city. Hernandez-Paniagua et al. (2015) recently analysed the long-term time series at the Royal Holloway site to study the long-term trends and seasonal variation in CO$_2$ mole fractions, which are driven by the variations in the biological uptake and of the anthropogenic activities underlying the city emissions. However, to our knowledge, these data have not yet been exploited using the inversion approach to quantify the city emissions. More recently, O'Shea et al. (2014) and Font et al. (2015) took airborne measurements of CO$_2$ mole fractions over London and combined these with box models to estimate vertical fluxes and a Lagrangian particle model to estimate the area ("footprints") corresponding to these fluxes. O'Shea et al. (2014) compared the flux estimates with eddy covariance flux measurements and the estimate of the city emissions from the 2009 UK National Atmospheric Emissions Inventory (NAEI) (NAEI, 2013). In the course of their analysis, Font et al. (2015) indicated that the uncertainties associated with footprint modelling are high and that there is a need to improve their protocol to separate the natural and anthropogenic CO$_2$ fluxes in their estimates, which is a traditional source of concern for the monitoring of anthropogenic emissions of CO$_2$ (Bréon et al., 2015). Regular aircraft campaigns could provide a good sampling of transitory city emissions, but the continuous monitoring of these emissions would likely have to rely on continuous measurements from ground-based stations. To our knowledge, there have been few attempts to monitor the CH$_4$ emissions of the London area using atmospheric measurements (Lowry et al., 2001; O'Shea et al., 2014).

In this context, we made quasi-continuous measurements of CO$_2$, CH$_4$ and CO during 2012 at four sites in the London area (two inner city sites – Hackney and Poplar; one suburban site – Teddington; and one rural site outside the urban area – Detling) using sensors located at 10–15 m above ground level. We assess the ability of a kilometre-resolution transport model driven by a kilometre-resolution emissions inventory to simulate these CO$_2$ and CH$_4$ measurements. The aim is to understand whether such measurement sites are ultimately suitable for use in a flux inversion scheme based on the kilometre-resolution model. This study investi-

gates the importance of different sources of discrepancies between observed and simulated GHG mole fractions (henceforth "model–data discrepancies"). By decomposing the discrepancies depending on their different sources, we attempt to isolate and exploit the part of the discrepancies that are due to the errors in the estimates of the urban emissions. We focus on the following sources of uncertainties and limitations when simulating the CO$_2$ and CH$_4$ measurements in the London area with the model, which we can assume to be significant sources of model–data discrepancies along with the errors in the estimate of the urban emissions:

1. The differences of representativity in terms of spatial scale between the model and the measurements: near-ground sites could be highly sensitive to very local emissions, i.e. at scales smaller than those represented by the model.

2. Uncertainties in the modelled meteorological conditions, in particular in the wind speed and direction and in the mixing layer height above the city.

3. Uncertainties relating to both the conditions at the model domain boundaries and to the modelling of the fluxes outside of the London area, which can influence the concentrations in the London area.

4. In the case of CO$_2$, uncertainties related to remote or near-field natural fluxes.

We introduce the measurement sites and model configuration in Sect. 2. In Sect. 3 we first consider issues of spatial representativity (Sect. 3.1) and then the ability of the model to simulate the diurnal cycle of mixing layer height, CO$_2$ and CH$_4$ (Sect 3.2). In Sect. 3.3 we compare winds simulated by the model with measurements at two surface meteorological stations. In Sect. 3.4 we examine the day-to-day variations in measured and modelled CO$_2$ and CH$_4$. We attempt to remove the influence of the remote fluxes and conditions by considering gradients in CO$_2$ and CH$_4$ across the city in Sect. 3.5, and then take the wind direction into account when selecting the gradients (Sect. 3.6). Finally, we evaluate the modelled fossil fuel CO$_2$ using a simple method to estimate the anthropogenic component of the observed CO$_2$ mole fractions based on the simultaneous CO measurements (Sect. 3.7). A summary and discussion of the overall findings of the research is then given in Sect. 4.

2 Methodology

2.1 London emissions inventory for CO$_2$ and CH$_4$

As context for the location of the in situ measurements, and to provide an estimate of the emissions applied within the model, we utilise the UK NAEI (NAEI, 2013), including a mapping of CH$_4$ sources from Dragosits and Sutton (2011).

The NAEI provides annual gridded emission data for a wide range of atmospheric pollutants and GHGs with a sectorial distribution by the main types of emitting activities: agricultural soil losses, domestic (commercial, residential, institutional) combustion, energy production, industrial combustion, industrial production processes, offshore own gas combustion, road transport, other transport, solvent use, waste treatment and disposal and (for CH_4 only) agricultural emissions due to livestock and natural emissions. Major CO_2 and CH_4 point sources (comprising large power and combustion plants) are also listed and localised individually. Significant sources of all these sectors apart from the offshore own gas combustion occur in the London urban area or in its immediate vicinity. The methodology applied to derive these gridded maps is described in Bush et al. (2010) and Dragosits and Sutton (2011).

The most up-to-date published emissions estimates available from the NAEI at the time of this study were for 2009. The CO_2 emissions for the region around London are shown at 2 km resolution (the resolution of simulated transport; see Sect. 2.4) in Fig. 1 along with the position of the measurement stations (Sect. 2.2). In the vicinity of London, nearly all point sources of CO_2 are related to combustion processes with emissions from high stacks and through warm plumes. The 10 largest emitters in the domain defined by Fig. 1 are power stations, which represent nearly 27 % of the emissions in this domain.

2.2 GHG measurement site locations and characteristics

The four measurement sites were located in and around London to sample air masses passing over London at various levels of sensitivity to urban emissions (in the city centre, suburban and rural areas). Note that no formal quantitative network design was applied beforehand to select the optimal location of the stations for their ability to constrain the emissions of London. The station locations were chosen based on the configuration of the emissions given by the inventory maps and the availability of suitable locations for installation and maintenance of the instruments.

The site locations are shown in Fig. 1 and were operational between June and September 2012. The two urban sites of Hackney and Poplar were located in central London, 6 km apart from each other and to the north-east of the main area of emissions (Hackney at 51°33′31.45″, −0°3′25.44″; Poplar 51°30′35.67″, −0°1′11.33″). The suburban site was located in Teddington (51°25′13.63″, −0°20′21.15), 17 km south-west of Central London. The location of this site was chosen a priori to allow the analysis of the gradient due to the city emissions when the wind blows from the south-west. This is usually the case and 52 % of the wind directions measured at Heathrow Airport (see Sect. 2.5) during the period July–September 2012 (i.e. our study period) were from the south-west sector. The fourth site was located in Detling,

Kent (51°18′28.44″, 0°34′57.36), in a rural area approximately 50 km from the inner city and was selected to help to detect the influence of remote fluxes on the GHG mole fractions over the city.

The measurement stations at Hackney and Poplar were located on the rooftop of a college and a primary education school respectively. The inlets for each of these sensors were placed approximately 10 m above street level and approximately 2 m above the rooftop level. The NAEI emissions map (Fig. 1) shows substantial CO_2 sources west of the Poplar and Hackney sites, relating to the city centre.

The site in Teddington was located on top of a building approximately 15 m from ground level. Teddington is referred to in this study as a suburban site, due to its location in a residential area beside Bushy Park. Bushy Park represents a large area of vegetation cover surrounding the site to the east, south and west with residential and commercial land use located to the north. The site in Detling was located on the top of a 10 m mast at an established air quality measurement site in a pasture field approximately 2 km from the nearest major roads.

2.3 GHG measurements

Continuous measurements of CO, CO_2, CH_4 and water vapour were taken between 1 June and 30 September 2012 for the Hackney, Poplar and Teddington sites and 5 July to 30 September 2012 at Detling. Each site was instrumented with a G2401 Picarro cavity ring-down spectroscopy (CRDS) instrument that logged data every 5 s and sent data files each hour to a remote server.

All sensors across the network were manually calibrated on an approximately 2-weekly basis using the same gas standards, ensuring the consistency of the measurements from different sites. The sensors were calibrated for linearity, repeatability of measurements (for zero and span gases, i.e. respectively with concentrations zero and ambient concentration gas) and drift in the field and in the laboratory prior to deployment. The synthetic standards including the zero and span gases were prepared by National Physical Laboratory (NPL) as described in Brewer et al. (2014) with mole fractions close to those of atmospheric ambient air (379 ± 0.95 parts per million (ppm) for CO_2 and 1800 ± 5 parts per billion (ppb) for CH_4; uncertainties are expressed as 1σ standard deviations, SD). A higher than ambient concentration of CO was used as the standard gas (9.71 ± 0.015 ppm to be compared with the CO measurements of this study, which range between 0.1 and 0.9 ppb), because of the unavailability of low CO standards at the time of the experiment, leading to high uncertainties in CO measurements in ambient air. However, the linearity of the G4201 CRDS has been evaluated by Zellweger et al. (2012) from 0 up to 20 ppm and their results show that the CRDS analyser remains linear in this range of concentrations.
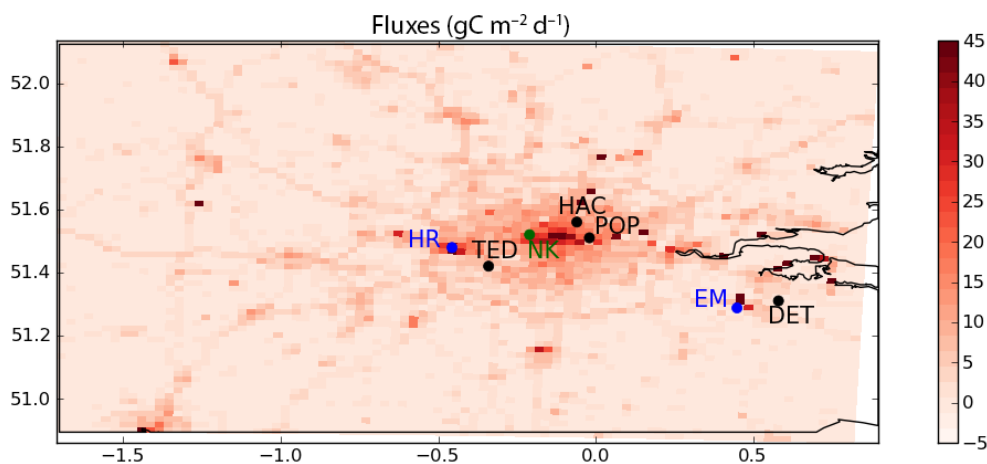
Figure 1. Map of the spatially derived (at 2 km resolution) CO_2 fossil fuel emissions inventories ($gC\,m^{-2}\,d^{-1}$) for the London section of the model domain, indicating the location of the four GHG measurement stations (black), the two meteorological sites Heathrow (HR) and East Malling (EM) (blue) and the North Kensington lidar site (NK, green). Dark red corresponds to relatively high CO_2 values (upper limit of $45\,gC\,m^{-2}\,d^{-1}$) and light pink to relatively low (uptake) CO_2 values (lower limit of $-5\,gC\,m^{-2}\,d^{-1}$).

To quantify possible biases, and consistent with the recommendation from the World Meteorological Organization (WMO) Expert Group, the design of the experiment should have included regular measurements of a calibrated target gas. However, the fact that we were using similar analysers at the four stations, operated with the same protocols and calibrated with a single reference scale, reduced the risk of systematic biases between the sites. The high 1σ uncertainties in the molar fraction of the gases used for the calibration result in unknown (positive or negative) biases that are common to all sites for the measurement period since the same gas cylinders were used for all stations throughout the period (the calibration error due to uncertainty in the calibration gas depends on the ambient concentration, but this dependence is such that the resulting variability of the calibration error is negligible compared with the variability of the concentrations in time or between sites). For this reason, the calibration biases mostly cancel out when analysing gradients of ambient molar fractions between the different sites of the network (this may not hold for higher molar fractions). This bias precludes, however, the use of this network in combination with other stations that have a different calibration standard.

In addition, the measurement error had a random component of SD 0.3 ppm for CO_2, 8 ppb for CH_4 and 15 ppb for CO. This error budget includes drifts and variability in readouts when measuring zero and span gases, as well as the applied correction for water vapour on the CO_2 and CH_4 channels. Such a correction was applied because the airstream to the Picarro CRDS was not dried. In practice, the measurements of CO_2 and CH_4 were taken from the dry channel of these analysers to which a default correction had been applied for variability due to water vapour (Rella et al., 2013). The uncertainty associated with applying the water vapour correction to this type of instrument, for an H_2O content of

1.5 %, was estimated to be 0.05 ppm for CO_2 and 1 ppb for CH_4 (Laurent et al., 2015). No water correction was applied for CO. Expressed as a percentage of the mean measured concentration throughout the measurement period, the total measurement uncertainties (root sum square, RSS, of the bias and random errors) are 0.3, 0.7 and 21 % for CO_2, CH_4 and CO respectively.

Data were calibrated using the standard gas cylinder values, and provided as 15 min averages by NPL. Calibration episodes were removed from the final data set. The Teddington sensor was inactive between 6 and 12 July due to sample pump failure and there were a small number of missing days at Detling (due to power outage) and at Poplar (for unknown reasons). There were few missing data at the Hackney site. The 15 min data from the measurement sites were aggregated by averaging into hourly time intervals for comparison with the hourly output from the model. If fewer than four 15 min data points were available for any given hour (usually as a result of periodic data scan by the Picarro analyser or return to functionality after a calibration event or instrument downtime), the corresponding model and measurement hourly averages were removed from the analysis to maintain consistency between the model and data hourly averaged values.

2.4 Simulation of the atmospheric transport of CO_2 and CH_4

To model the transport of CO_2 and CH_4 mole fractions over London, we used a "south of England" configuration of the mesoscale atmospheric transport model CHIMERE (Schmidt et al., 2001). This model has already been used for CO_2 transport and flux inversion at regional to city scale (Aulagnier et al., 2010; Broquet et al., 2011; Bréon et al., 2015). The

domain over which CHIMERE was applied in this study (area ~ 49.9–$53.2°$ N, -6.4–$2.4°$ E) covers the whole south of England to minimise the impact of defining model boundary conditions using coarser model simulations close to the measurement sites. Additionally, the boundaries were positioned as much as possible in the seas (instead of set across southern England), in particular the western boundary, from which the dominant winds flow over England. However, the northern boundary crosses England and the south-eastern part of the domain overlaps a small part of northern France.

The model has a regular grid with 2 km horizontal resolution and 20 vertical levels from the ground up to 500 hPa (with ~ 20–25 m vertical resolution close to the ground). CHIMERE is driven by atmospheric mass fluxes from the operational analyses of the European Centre for Medium-Range Weather Forecasts (ECMWF) at 3 h temporal resolution and ~ 15 km horizontal resolution (which are interpolated linearly on the CHIMERE grid and every hour). In this study, these mass fluxes were processed before their use in CHIMERE to account for the increased roughness in cities and in particular in London: the surface wind speed was decreased proportionally to the fraction of urban area in each model 2 km $\times$ 2 km grid cell (i.e. it is set to 0 for grid cells entirely covered by urban area, set to the value from ECMWF for grid cells with no fraction of urban area, and, in a general way, set to the product of the fraction of non-urban area in the grid cells times the value from ECMWF). The fraction of urban area within each 2 km $\times$ 2 km grid cell was derived from the land cover map of the Global Land Cover Facility (GLCF) 1 km $\times$ 1 km resolution database from the University of Maryland. This database is based on the methodology of Hansen and Reed (2000) and Advanced Very High Resolution Radiometer (AVHRR) data. The decreases in horizontal wind speed are balanced by an increase in the vertical component of the wind. However, the current configuration does not account for the urban heat island effect either in the ECMWF product or in the processing of this product before its use by CHIMERE.

The simulations were initialised on 15 April 2012. For the CO_2 simulations, the initial mole fractions and the open boundary conditions (at the lateral and top boundaries of the model) were imposed using simulated CO_2 from the Monitoring the Atmospheric Composition and Climate Interim Implementation (MACC-II, 2012) forecasts at ~ 80 km resolution globally (Agustí-Panareda et al., 2014). The MACC-II forecast was initiated on 1 January 2012 with online net ecosystem exchange (NEE) from the CTESSEL model (see the description below of the estimate of natural fluxes used for the CHIMERE simulations) and prescribed fossil fuel CO_2 emissions and air–sea fluxes, and is not constrained by CO_2 observations. For the CH_4 with CHIMERE, the initial and boundary conditions were imposed homogeneously in space and time to be equal to 1.87 ppm, according to the typical mole fractions measured at the Mace Head atmospheric

measurement station in 2012 (NOAA, 2013). The top boundary conditions were set to a smaller value: 1.67 ppm.

Anthropogenic emissions of CO_2 and CH_4 were prescribed to CHIMERE within its domain using the NAEI, described in Sect. 2.1. Three-dimensional hourly emissions for CO_2 and CH_4 were interpolated from this inventory on the 2 km horizontal resolution model grid. The derivation of the emissions for the UK based on the NAEI included injection heights for major point sources and temporal profiles (see below for details on the definition of injection heights and temporal profiles). The CO_2 emissions for the small part of France appearing in the domain were derived from the Emission Database for Global Atmospheric Research (EDGAR, 2014) at $0.1°$ horizontal resolution for the year 2008. Injection heights and temporal variations were ignored for this part of France, which is assumed to have little impact on the simulation of CO_2 in London because of the distance between these two areas and since the dominant wind blows from the south-west.

The definition of injection heights can have a large impact when modelling the transport of CO_2 mole fractions from combustion point sources (Bieser et al., 2011). Many parameters underlying the effective injection heights for each source are not available (e.g. the stack heights, the flow rate and the temperature in the stacks). Furthermore, this study focuses on data during summer and, as indicated later, during the afternoon, when the troposphere is well mixed, so that the impact of the injection heights is minimum. Therefore, we derived approximate values for these heights as a function of the sectors associated with the point sources only, and based on the typical estimates by sector for nitrogen oxide gases (NO_x), CO and SO_2 (and for neutral atmospheric temperature conditions) from Pregger and Friedrich (2009). The resulting injection heights for the emissions listed as point sources by the NAEI (other emissions were prescribed at ground level) ranged from the second vertical CHIMERE level (~ 25 to 55 m a.g.l.) for the smallest industrial and commercial combustion plants to the 8th vertical CHIMERE level (~ 390 to 490 m a.g.l.) for the power stations. All CH_4 emissions sources were prescribed at ground level.

The variations in CO_2 and CH_4 in time are strongly driven by those of the emissions at the hourly to the seasonal scale (Reis et al., 2009). In the modelling framework of this study, temporal profiles were derived for the three sectors of CO_2 emissions with the largest variations in time: road transport, power generation in large combustion plants, and residential and commercial combustion. They were based on Reis et al. (2009) using data from 2004 to 2008. These sectorial profiles were applied homogeneously in space for the whole south of England. For road transport, the temporal profiles were based on the product of monthly weights for a typical year, daily weights for a typical week and hourly weights for each day of the week (with two maxima during week days and one maximum for Saturdays and Sundays) derived from statistical data about the variations in traffic flows in

the UK. For the power generation and residential and commercial combustion, only monthly variations were considered based on the consumption for typical years. Previous studies have diagnosed some seasonality for CH_4 emissions (Lowry et al., 2001; McKain et al., 2015). As examples of the potential explanations for this phenomenon, the seasonality of the gas consumption for heating (with large consumption for lower temperatures, especially in winter) could drive seasonal variations in the gas leakage (Jeong et al., 2012), and the seasonal variations in the meteorology (pressure, humidity, temperature) could impact the decomposition and release of CH_4, and thus the emissions, from the waste storage and waste treatment sector (Börjesson and Svensson, 1997; Masuda et al., 2015; Abushammala et al., 2016). However, characterising such seasonal variations is a difficult task, which may vary substantially depending on the sectors and cities. To our knowledge, there are no studies on which we could build reliable temporal profiles for the CH_4 emissions in London, and we thus did not attempt to derive them. Instead, we set the CH_4 emissions constant in time.

Natural fluxes of CO_2 were taken from the 15 km resolution NEE product from ECMWF (Boussetta et al., 2013), which is calculated online by the CTESSEL land-surface model coupled with the ECMWF numerical weather prediction model. The CTESSEL model does not have a specific implementation for urban ecosystems and due to its moderate 15 km horizontal resolution, we cannot expect this model to provide a precise representation of the role of ecosystems within London.

Ocean fluxes for both gases within the domain were ignored because they are assumed to be negligible at the timescales considered in this study (Jones et al., 2012). At the spatial and temporal scales considered in this study, the loss of CH_4 through chemical reactions is also negligible and was thus ignored here.

The model tracks the transport of the total CO_2, but also of its different components separately: CO_2 from the boundaries (BC-CO_2), from the NEE (BIO-CO_2) and from fossil fuel emissions (FF-CO_2). The model does not track CO mole fractions; however, the CO measurements are used to evaluate the FF-CO_2 in Sect. 3.7.

The 15 km resolution of the ECMWF analyses, used as meteorological forcing for CHIMERE, yields relatively uniform wind speed and direction at the city scale. The interpolation of this product on the 2 km CHIMERE grid is compared with the observations from surface meteorological sites located in and around London in Sect. 3.3.

2.5 Meteorological measurements

An important contribution to model–data discrepancies can arise from errors in the representation of meteorological conditions; particularly wind speed and direction, and mixing layer height. To evaluate the errors in the meteorological forcing of CHIMERE, hourly observations of wind speed

and direction were collected from the UK Met Office Integrated Data Archive System (MIDAS) (Met Office Integrated Data Archive System (MIDAS) Land and Marine Surface Stations Data (1853–current)", 2012). The measured wind data were obtained for 10 m a.g.l. at Heathrow Airport, London (51° 28′43.32″, −0°26′56.54″), and East Malling, Kent (51° 17′15.36″, 0°26′54.24″). East Malling is located 6 km from the Detling site and Heathrow is located 7 km from the Teddington site and 18 km from the Hackney and Poplar sites. The locations of the meteorological sites are shown in Fig. 1.

Observed winds at East Malling were compared with winds from ECMWF (interpolated on the CHIMERE grid) at the lowest level (0–25 m) and at the corresponding horizontal location of the CHIMERE grid. Observed winds at Heathrow were compared with the next CHIMERE level up (25–50 m) because the urban roughness correction had been applied to the lowest level. This avoids strong biases in the model–data comparison that would arise because the urban roughness correction was necessarily applied in a homogenous way for the corresponding model grid cell, while, in reality the site is not located within the urban canopy.

Hourly mean mixing height measurements were collected from a Doppler lidar that was located on the grounds of a school in North Kensington (51°31′13.97″, −0°12′50.85″) as part of the ClearfLo project (Bohnenstengel et al., 2015). The limited sampling rate of the lidar was accounted for using a spectral correction method described in Barlow et al. (2014) and Hogan et al. (2009). Mixing heights were calculated based on a threshold value of the vertical velocity variance, which was perturbed between 0.080 and 0.121 $m^2 s^{-1}$, to check the sensitivity of calculated mixing heights to the threshold, which is an approximate parameter for this computation. Mean, median, and 5th and 95th percentile values were calculated for each hour based on these perturbations, and account for both measurement and method uncertainties (Barlow et al., 2014; Bohnenstengel et al., 2015). Based on the 5th and 95th percentile data averaged across all data for each hour, estimated measurement and method uncertainty was between 53 and 299 m throughout the daily cycle, with the highest uncertainties usually overnight. These measurement uncertainties are small when compared with the amplitude of the observed diurnal cycle shown in Fig. 3a. Lidar data were available for the period between 23 July 2012 and 17 August 2012 and were compared with the modelled boundary layer height (diagnosed in the ECMWF forecast using a critical value of 0.25 for the bulk Richardson number) at North Kensington during this period.

3 Results and discussion

The data used for all statistical diagnostics of the model–data discrepancies in this section (including the wind roses and mean diurnal cycles in Figs. 2 and 3) are for the period 5 July
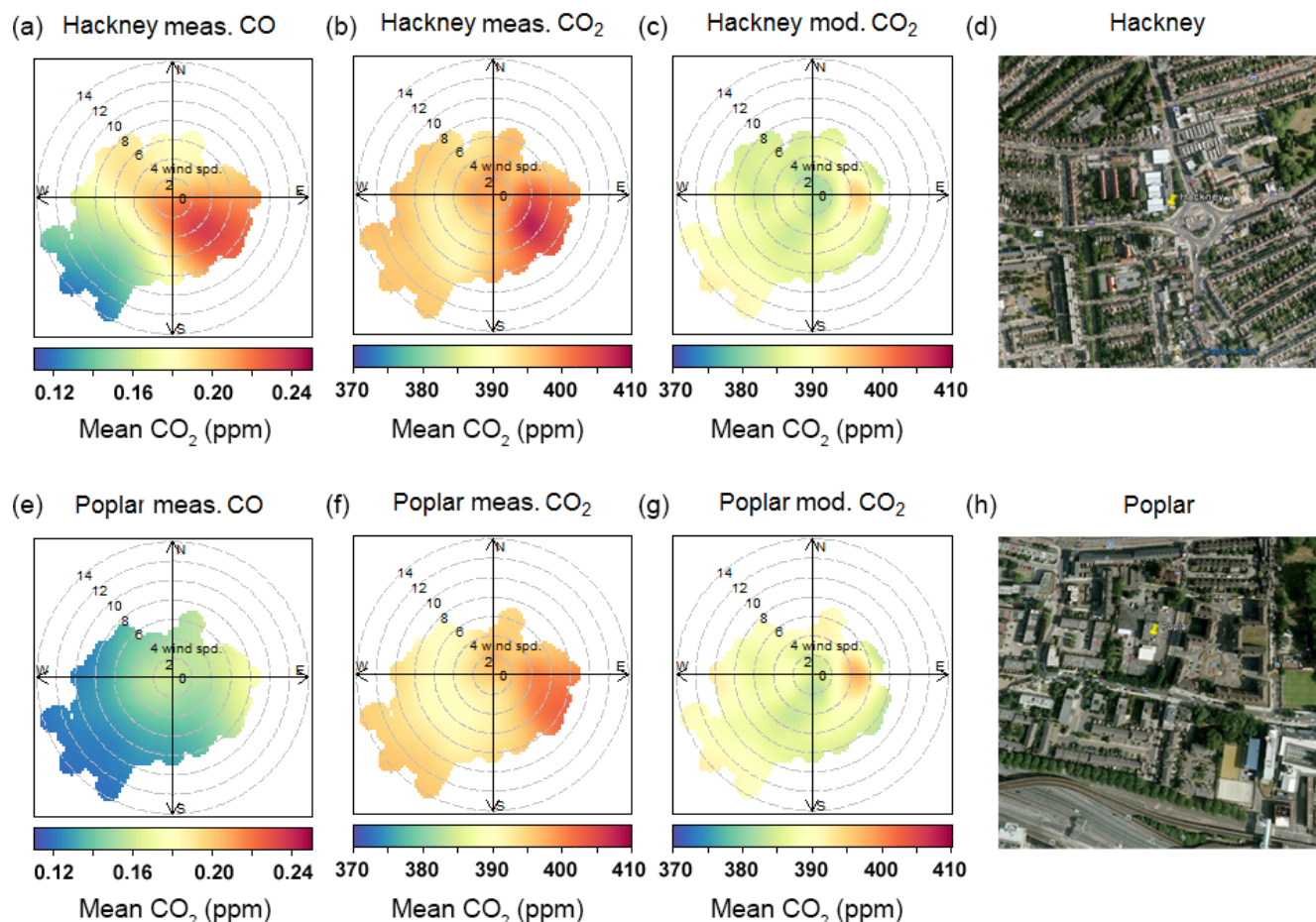
Figure 2. Wind roses for each urban measurement site incorporating hourly data for wind speed, wind direction (Heathrow measured data) and CO_2 mole fraction between the hours 12:00 and 17:00 UTC for **(a)** observed CO mole fractions at Hackney, **(b)** observed CO_2 mole fractions at Hackney, **(c)** modelled CO_2 mole fractions at Hackney, **(d)** a map (©2012 Google Imagery and Bluesky, the GeoInformation group) of the immediate vicinity of the Hackney site, **(e)** observed CO mole fractions at Poplar, **(f)** observed CO_2 mole fractions at Poplar, **(g)** modelled CO_2 mole fractions at Poplar and **(h)** a map (©2012 Google Imagery and Bluesky, the GeoInformation group) of the immediate vicinity of the Poplar site. The colours on the wind roses show the gas mole fraction (parts per million, ppm) with the radius corresponding to the magnitude of the wind speed (m s^{-1}) and the azimuthal angle to the wind direction (° N). Red corresponds to relatively high concentrations and blue to relatively low concentrations within the given scale of each gas (min = 0.11 parts per billion (ppb) and max = 0.25 ppb for CO, and min = 370 ppm, max = 410 ppm for CO_2).

to 30 September 2012 since data were available at all GHG sites during this period. The analyses of model–data discrepancies in GHG mole fractions utilise the hourly average of the 15 min aggregate measurements (Sect. 2.3) and the analyses of meteorological measurements relate to hourly data for the same period. However, some of the figures with time series of the GHG concentrations display the GHG available data in June 2012 to provide indications that the behaviour of the model is similar between June and the following months. Hereafter, we use the term "signature" to refer to the positive or negative amount of atmospheric gas mole fraction (and to its spatial and temporal variations) due to a given flux (natural or anthropogenic surface source or sink over a given area

and over a given time period, or advection of an air mass from a remote area).

3.1 First insights on the influence of local sources on urban GHG measurements

We first consider the representativity of the CO_2 and CO at the urban sites by analysing them as a function of wind speed and direction. In particular, we try to give a first assessment of the weight in the measurements of "local" sources. By local sources, we refer to sources that are located at distances from the measurement sites that are shorter than the distances over which we can simulate the transport from these sources at the spatial resolution of our Eulerian model. This includes sources at less than 1–5 km from the measurement sites since
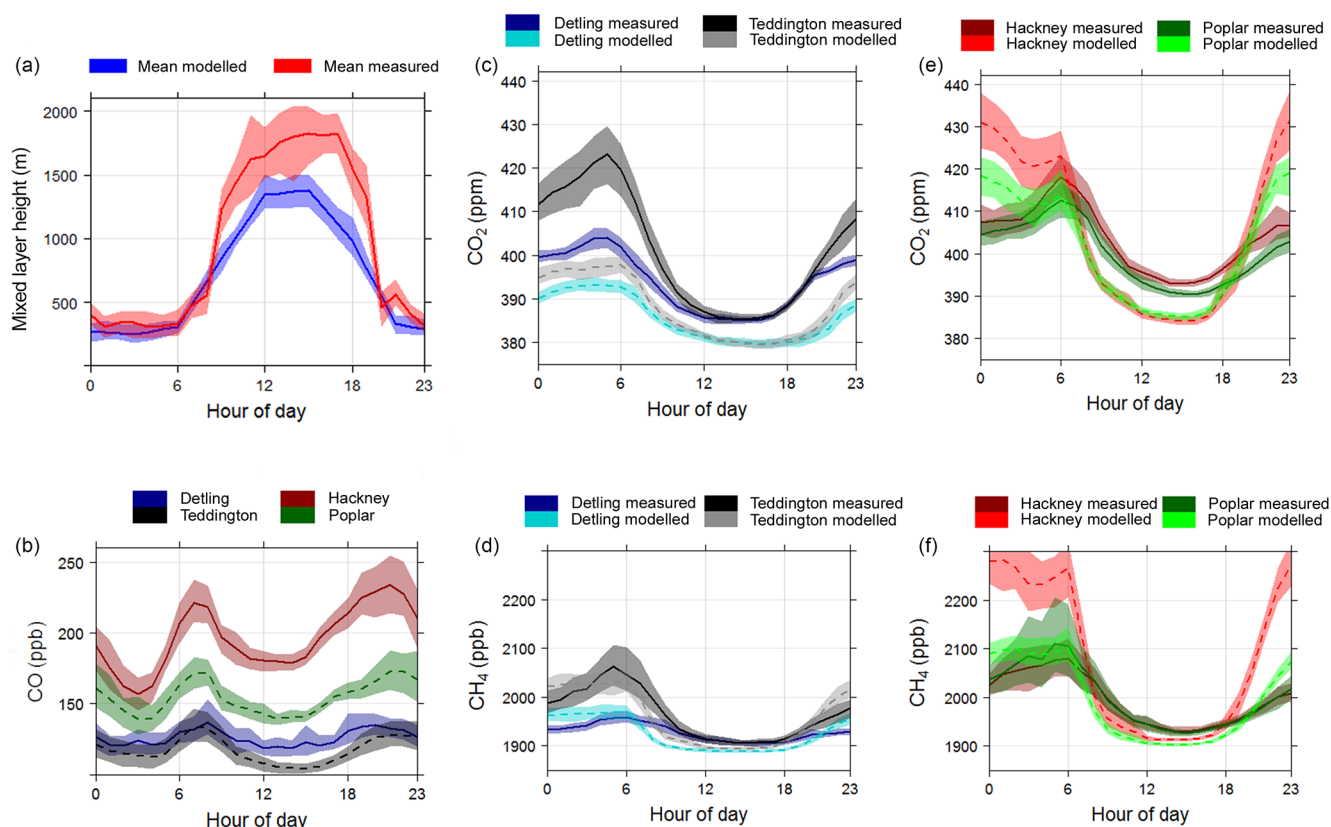
Figure 3. Mean diurnal cycles of **(a)** modelled (blue) and measured (red) boundary layer height and measured mean mixing layer height at North Kensington based on the spectral correction method described in Sect. 2.5, **(b)** measured CO mole fractions at the rural (Detling, blue), suburban (Teddington, black), and urban sites (Hackney, red; Poplar, green), **(c)** modelled (light shade) and measured (dark shade) CO_2 mole fractions at the rural (Detling, blue) and suburban (Teddington, black) sites, **(d)** modelled and measured (dark shade) CH_4 mole fractions at the rural (Detling, blue) and suburban (Teddington, black) sites **(d)** modelled (light shade) and measured (dark shade) CO_2 mole fractions at the urban (Hackney, red; Poplar, green) sites and **(f)** modelled and measured CH_4 mole fractions at the urban (Hackney, red; Poplar, green) sites. June data are excluded due to unavailability of data during this period at Detling. Shading represents an estimate of the 95 % confidence interval in the mean, related to the limitation of the sampling of the daily values at a given hour, assuming these values are independent (based on the division of 2 times their temporal standard deviation by the square root of the number of values).

the model has a 2 km horizontal resolution. Figure 2 shows wind roses at Hackney and Poplar for measured CO and CO_2, and modelled CO_2, alongside aerial images of the site locations. To reduce the influence of boundary layer variation on the measured and modelled mole fractions, and to anticipate the data selection on which the study will focus, we include measured and modelled data for the afternoon period only (see Sect. 3.2).

At Hackney there is an increase in measured CO and CO_2 mole fractions during periods of south-easterly wind (Fig. 2a and b). A busy roundabout is located approximately 10 m to the south-east of the Hackney site with an A-road running from north to south to the east of the sensor location (Fig. 2d). There is no increase for south-easterly winds when analysing modelled CO_2 (Fig. 2c), suggesting that the observed increase in the measurements could be related to the roundabout whose specific influence cannot be represented at the 2 km resolution in the model.

At Poplar, the measured CO and CO_2 is more uniform than at Hackney (Figs. 2e and f). It is still higher in the east, but there is no visible signature of the busy roads to the north and south of the site (Fig. 2h). The modelled CO_2 at Poplar (Fig. 2h) is very similar to that of Hackney (Fig. 2c), which can be explained by the proximity between the two corresponding model grid cells (Fig. 1). This supports the earlier assumption that the high mole fractions obtained at Hackney for south-easterly winds are related to a local source. These analyses also raise a more general assumption that while the model simulates the signature of emissions at a relatively large scale (due to handling emissions and transport at 2 km resolution and with significant numerical diffusion) in the area of these 2 sites, there are likely local-scale unresolved emissions strongly influencing observed CO_2 at both urban sites.

At both urban sites the observed CH_4 wind roses are very similar, showing increased mole fractions towards the east

of the sites (data not shown); however, mole fractions are greater in magnitude at Poplar than at Hackney. Similarly to CO_2, the model simulates lower CH_4 mole fractions than observed, with a similar distribution at both sites. The stronger similarity between the wind roses at the two sites when considering CH_4 measurements than when considering CO_2 measurements could be explained by the absence of strong CH_4 local sources in the vicinity of the measurement sites. The NAEI does not locate any major waste treatment facility at less than 5 km from these sites and it assigns a level of emissions from the other sectors (which are characterised by diffuse sources in the inventory) for this vicinity that is similar to the general level of CH_4 emissions in the London urban area. Local CH_4 leaks from the gas distribution could occur and impact the measurements, but this analysis does not highlight such local sources.

Despite the potential influence of local sources that are unresolved by the transport model, we attempt, in the following sections, to understand and decompose the large discrepancies between the model and the measurements illustrated in Fig. 2. The objective is to analyse whether one can identify the discrepancies due to errors in the emissions at scales larger than $2 \text{ km} \times 2 \text{ km}$, which should give insights on the potential for applying atmospheric inversion.

3.2 CO_2, CH_4 and mixing layer mean diurnal cycles

The mean observed and modelled diurnal cycles of the CO, CO_2 and CH_4 mole fractions at the four GHG measurement sites and the mixing layer height at North Kensington (see Sect. 2.5) are presented in Fig. 3. The amplitude of the mean diurnal cycle in mixing layer height (Fig. 3a) is approximately 1500 m, typical of summer convective conditions in an urban area (Barlow et al., 2014).

Observed CO_2 mole fractions at all sites follow a typical mean diurnal cycle (Fig. 3) with maximum mole fractions in the early morning (approx. 05:00 UTC) and minimum mole fractions during the afternoon (approx. 15:00 UTC), which can be related to the typical variation in mixing height (Fig. 3a), and in vegetation CO_2 exchanges (with photosynthesis and a CO_2 sink during daytime but CO_2 emissions during night-time) during a daily cycle. The early morning peak in CO_2 mole fractions occurs on average an hour later at the inner city sites (06:00 UTC) compared with the rural and suburban sites (05:00 UTC) as shown in Fig. 3c and e. This may be due to the signature of working-week urban emissions with a peak in traffic around 06:00 to 09:00 UTC. This is supported by large observed CO mole fractions at the urban sites with substantial early morning and evening peaks (Fig. 3b). The peak in CH_4 measured mole fractions occurs at around 06:00 UTC at all sites (Fig. 3d and f).

At all sites the model underestimates by 1 to 5 % (by 5 to 9 ppm for CO_2 and by 13 to 29 ppb for CH_4) the mean observed CO_2 and CH_4 mole fraction during the afternoon hours (12:00 to 17:00 UTC), with the highest biases at Hack-

ney for CO_2 and at Poplar for CH_4 (see the model–data biases for this period in Table 1). This underestimation is consistently larger than the confidence intervals for the averaging (associated with the limited time sampling) indicated throughout Fig. 3. The underestimation continues throughout the diurnal cycle at Detling and Teddington (Fig. 3c and d); however, at the urban sites (Fig. 3e and f), the night-time (00:00 to 05:00 UTC) CO_2 and CH_4 mole fractions are considerably larger in the model than in the observations. This leads to excessively strong diurnal variations at the urban sites, with the exception of CH_4 at Poplar (Fig. 3f).

On average, mixing layer height is underestimated in the model at North Kensington by approximately 13 % (46 m) of the equivalent lidar measurement during the night and 33 % (583 m) during the afternoon (Fig. 3a). There is a high daily variability in the mixing layer height model–lidar measurement discrepancies (with a 454 m SD in the 12:00–17:00 UTC period and a 394 m SD in the 00:00 to 05:00 UTC period), and thus this underestimation is not systematic (see Sect. 3.4). However, this may still explain the overestimation of mole fractions at the urban sites during night-time but cannot explain the underestimation of CO_2 and CH_4 mole fractions during the afternoon.

Accurate modelling of the boundary layer height in meteorological models is an on-going concern, particularly in urban areas (Gerbig et al., 2008; Lac et al., 2013) and description of nocturnal stratification is weak in atmospheric transport models (Geels et al., 2007). During the night there can be a considerable urban heat island in London as shown for North Kensington and rural Chilbolton by Bohnenstengel et al. (2015). The model used in our study does not currently have an urban land-surface scheme capable of reproducing the urban heat island effects on atmospheric transport (Sect. 2.4). This may explain the different sign of the model–data discrepancies during night-time between the urban sites and the other sites. We thus restrict the remaining analyses in this paper to the period between 12:00 and 17:00 UTC, wherein we can expect the boundary layer to be well developed, to have a stable height and to exert minimum influence on the variations in gas mole fractions (Geels et al., 2007; Göckede et al., 2010).

3.3 Comparison between modelled and measured winds

This section focuses on the horizontal wind, which is a critical driver of day-to-day variations in GHG mole fractions. We aim to validate the model wind forcing through comparison with meteorological sites described in Sect. 2.5. The analyses (using hourly data) of measured and modelled wind are restricted to between 12:00 and 17:00 UTC because all further GHG analyses are focused on this afternoon period (Sect. 3.2).

At East Malling, on average, the model underestimates wind speed by 0.50 m s^{-1} (12 % of the observation mean)

Table 1. Summary of systematic and random errors of hourly measurements (see Sect. 2.3) and of the hourly model–data discrepancies using data between 12:00 and 17:00 UTC during July to September 2012. Values are given for CO_2 (CH_4 in brackets) in parts per million (ppm) and parts per billion (ppb) for CH_4. SD denotes standard deviation; RMS denotes root mean square.

Error type	Measurement error	Model–data discrepancies			
		Detling	Hackney	Poplar	Teddington
Bias	SD of bias: 1.0 (5)	−5.3 (−19.0)	−9.1 (−20.7)	−5.5 (−28.6)	−5.7 (−13.3)
SD	0.3 (8)	6.5 (27.4)	7.3 (43.2)	7.1 (46.9)	7.1 (29.3)
RMS	–	8.4 (33.3)	11.7 (47.9)	9.0 (54.9)	9.1 (32.2)

and wind direction by 6.90° (defining positive angles clockwise hereafter). The RMS of the hourly model–data discrepancies is $1.10\,\mathrm{m\,s^{-1}}$ for wind speed and 26° for wind direction. At Heathrow Airport, there is an average positive bias of $0.37\,\mathrm{m\,s^{-1}}$ (7 % of observation mean) and 5° for wind speed and direction respectively (RMS model–data discrepancies of $1.27\,\mathrm{m\,s^{-1}}$ and 2.24° for wind speed and direction respectively). Some of this discrepancy may arise from the necessity of comparing the 25–50 m average wind data from the model to the 10 m height measurements at the Heathrow meteorological station.

It is highly difficult to translate such statistics of the errors on the wind into typical errors on the simulation of the GHG concentrations at the GHG measurement sites since there is a complex relationship between them, which strongly depends on the specification of the local to remote emissions, and on the spatial distribution of the errors in the meteorological parameters or in these emission estimates at the local to larger scales. The overestimation of the wind speed in the urban area, unlike the underestimation of the mixing layer height, could partly explain the underestimation of the afternoon GHG concentrations at the urban sites since it should lead, on average, to an underestimation of the signature of the urban emissions. However, such an impact of the 7 % overestimation of the urban wind speed cannot explain, by itself, the 5 to 9 ppm (21 to 29 ppb) underestimation of the urban CO_2 (CH_4) afternoon concentrations since the average differences between the urban and rural or suburban concentrations during the afternoon do not exceed 10 ppm and 30 ppb according to both the model and the measurements (Fig. 3).

Lac et al. (2013) employed the Meso-NH meteorological model at 2 km horizontal resolution with an urban surface scheme that models specific energy fluxes between urban areas and the atmosphere. Their modelled meteorology was compared with hourly meteorological measurements in the Paris region. They showed a typical bias of $0.8\,\mathrm{m\,s^{-1}}$ for wind speed and 20° for wind direction, which is larger than the agreement obtained here with the ECMWF winds driving CHIMERE at a native resolution of 15 km. Nehrkorn et al. (2013) found a wind speed bias of between −1 and $2.5\,\mathrm{m\,s^{-1}}$ and RMS of between 1 and $4\,\mathrm{m\,s^{-1}}$ when comparing the Weather Research and Forecasting (WRF) model at 1.33 km resolution over Salt Lake City, US, with an urban

land-surface scheme, to local hourly wind measurements. Therefore, the choice of a 15 km wind field to force the CHIMERE transport model over London does not seem to raise typical wind errors larger than when using a state-of-the-art meteorological model at typically 1 to 3 km resolution.

3.4 Daily CO_2 and CH_4 mole fractions during the mid-afternoon

The average CO_2 and CH_4 mole fractions for the afternoon of each day throughout the analysis period are presented in Figs. 4 and 5. Some data have been excluded from these analyses; we ignore hereafter, at a given site, any hour during which either modelled or measured data were not available. We have also excluded data from 29 August and 23 to 24 September since the model simulated very large GHG peaks on these days which do not occur in the data. Data from June have been excluded from the statistical analysis to maintain comparability with Detling at which data were not available during this month.

According to both the measurements and the model, there is an increase in both the mean value (typically by 7 ppm and 26 ppb according to the measurements) and variability (typically by 1 ppm and 16 ppb according to the measurements) of CO_2 and CH_4 mole fractions, from the rural and suburban Detling and Teddington sites (Figs. 4a, d, 5a and d) to the urban sites Hackney and Poplar (Figs. 4b, c, 5b and c). This can be explained by their relative distance to the main area of anthropogenic emission in the centre of London (Fig. 1) and due to the location of Teddington (Detling) to the south-west (south-east) of the London area, while the dominant wind directions are from the west. According to the model, in general, modelled CO_2 is lower than the signature of the Monitoring the Atmospheric Composition and Climate Interim Implementation (MACC-II) boundary conditions (BC-CO_2 in Fig. 4) at Detling and Teddington (by ∼ 3 ppm on average) since the negative signature of the CO_2 NEE is larger than the positive signature of the anthropogenic emissions between the model boundaries and these sites (see Fig. 4a and d). The London emissions between Detling or Teddington and Hackney or Poplar compensate for this decrease (see Fig. 4b and c) in such a way that CO_2 at Hackney and Poplar is gener-
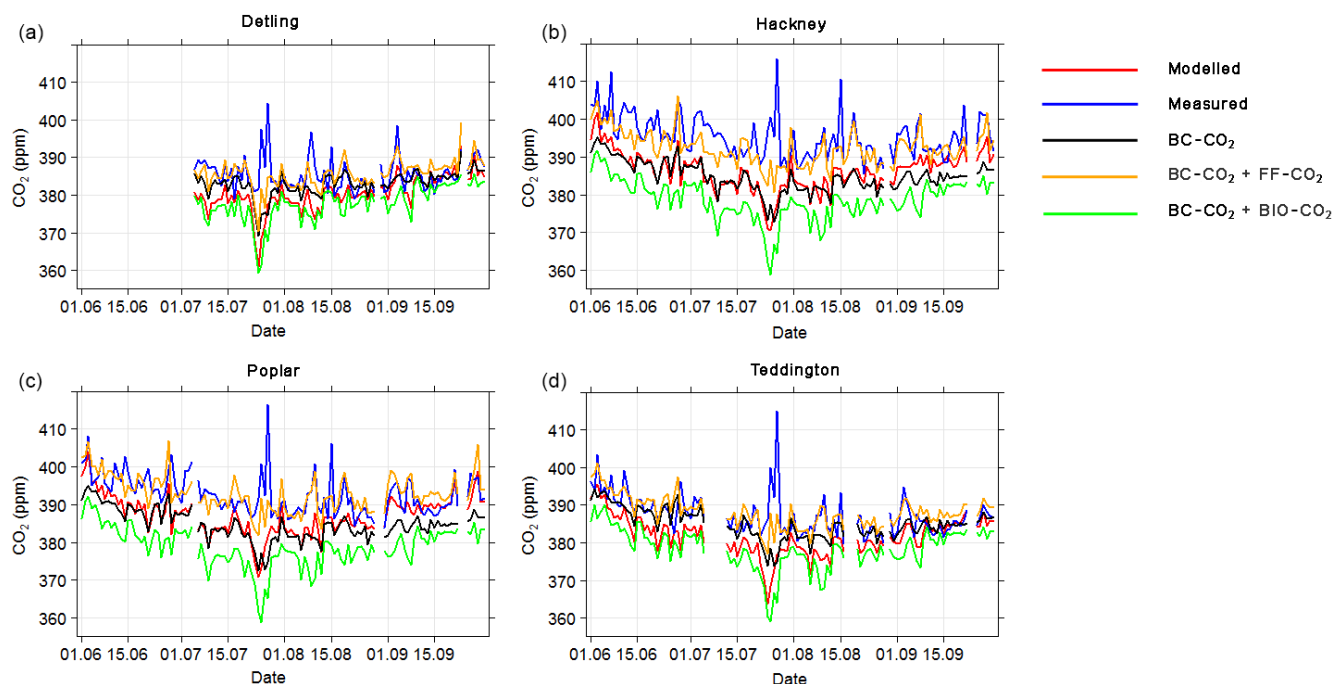
Figure 4. Time series of averages for the afternoon period (12:00 to 17:00 UTC) each day of modelled CO_2 mole fractions (red), measured CO_2 mole fractions (blue), modelled signature of the CO_2 boundary condition mole fractions from MACC-II (BC-CO_2, black), the modelled signature of the CO_2 fossil fuel emissions added to that of the boundary conditions (BC-CO_2+FF-CO_2, orange) and the modelled signature of the CO_2 NEE added to that of the boundary conditions (BC-CO_2+BIO-CO_2, green) at **(a)** Detling, **(b)** Hackney, **(c)** Poplar and **(d)** Teddington.

ally similar to BC-CO_2 (with less than 1 ppm difference on average over July–August), except in September, when it is higher (by ~ 5 ppm on average) because of the NEE being weaker in this month than during the previous months. Furthermore, the NEE and the anthropogenic emissions do not strongly alter the CO_2 variability from the boundary conditions and the correlation (R value) between the variations in modelled hourly CO_2 and those of hourly BC-CO_2 is high (between 0.75 and 0.85, depending on the site) even at urban sites. The modelled CH_4 time series, which uses a constant value at the boundaries, cannot show such a dependency on the model boundary conditions (Fig. 5).

Statistical comparisons between modelled and measured hourly CO_2 and CH_4 mole fractions are given in Table 1. While the magnitude of the SD of the model–data discrepancies is similar to that of the bias for CO_2, it is far larger than the bias for CH_4. The RMS of CO_2 model–data discrepancies is highest at Hackney (12 ppm) but similar at the other three sites (8 to 9 ppm, Table 1). Higher RMS of CH_4 model–data discrepancies are found at Poplar and Hackney (48 and 55 ppb) than at Teddington and Detling (32 and 33 ppb) (Table 1). The model–data discrepancies are substantially larger than measurement errors for both CO_2 and CH_4 (Table 1) so we can exclude measurement error as a key source of the discrepancies. The discrepancies should thus mainly be associated with representation errors (Sect. 3.1), transport er-

rors (Sect. 3.3), errors in the domain boundary conditions and in the prescribed fluxes within the domain and outside the London area, or with errors in the emissions prescribed in the London area (based on NAEI data; see Sect. 2.1). The model–data CO_2 or CH_4 hourly discrepancies at the urban sites during the afternoon are not significantly correlated (R values are between 0 and 0.2 for all cases) with the mixing layer height model–lidar measurement discrepancies at North Kensington (Sect. 3.2) or with the wind speed or direction model–data discrepancies at Heathrow Airport (Sect. 3.3).

Model–data correlations are significantly higher for hourly CH_4 (R values between 0.4 and 0.6, depending on the sites) than for hourly CO_2 (between 0. and 0.1). However, the amplitude of the variations in hourly CH_4 is strongly different between the model (whose SD is of 15.5 to 18.5 ppb depending on the sites) and the measurements (whose SD is of 32.8 to 51.5 ppb), which explains the very large model–data discrepancies given in Table 1. The potential impact of local CH_4 sources near the urban sites (see Sect. 3.1) cannot explain that these discrepancies are very high at Teddington and Detling even though they can explain that they are significantly larger at Hackney and Poplar. This suggests that the actual CH_4 conditions on the boundaries of the modelling domain may have a strong influence on the variations in mea-

sured CH_4, as for CO_2, but we miss it through the use of constant CH_4 boundary conditions in the model.

3.5 CO_2 and CH_4 gradients between pairs of sites

An increasing number of studies on the atmospheric monitoring of the city emissions focus on analysing and assimilating measurement gradients (Bréon et al., 2015; McKain et al., 2015; Turnbull et al., 2015; Wu et al., 2015; Staufer et al., 2016) rather than measurements at individual sites since it reduces the influence of the GHG fluxes that are outside the city of interest (of the model boundary conditions and of the fluxes that are outside the city but within the model domain when analysing model simulations). This approach assumes that such an influence has a large spatial and temporal scale and is therefore similar for different measurement sites in and around the city (Bréon et al., 2015). Here, the strong influence of boundary conditions on the modelled CO_2, and the potential issue raised by using a constant boundary condition for the CH_4 simulations, leads us to assume that uncertainties in both of the CO_2 or CH_4 boundary conditions can explain a large part of the substantial discrepancies between observed and modelled GHGs that are diagnosed at the four measurement sites. We thus analyse the CO_2 or CH_4 gradient between the urban sites and the rural or suburban sites. Because of this computation, the rural and suburban sites are called hereafter "reference sites". This analysis requires data at both the urban and the reference sites for a given hour and thus adds a new criterion to the data time selection already described and applied in Sect. 3.4. The gradients are henceforth described as follows: Hackney and Detling (HAC–DET), Hackney and Teddington (HAC–TED), Poplar and Detling (POP–DET) and Poplar and Teddington (POP–TED).

Figure 6 presents the daily afternoon mean gradients of measured and modelled CO_2 and CH_4 mole fractions (ΔCO_2 and ΔCH_4) alongside the daily afternoon mean gradient of modelled fossil fuel CO2 (FF-CO_2) and NEE (BIO-CO_2) components (ΔFF-CO_2 and ΔBIO-CO_2) from the model simulation. One can see from Fig. 6 that the modelled ΔCO_2 closely tracks modelled ΔFF-CO_2 (with R values of 0.80–0.95 depending on the selected pair of sites), while ΔBIO-CO_2 (the average of which is smaller than 0.9 ppm in absolute value between all pairs of sites) and the influence of the boundary conditions on these gradients (the average of which is smaller than 0.1 ppm in absolute value between all pairs of sites) are relatively small, compared with ΔFF-CO_2, particularly when Teddington is used as the reference site (Fig. 6). This strongly supports the assumption that the signature of boundary conditions and fluxes outside the London area operates on a large spatial and temporal scale and is therefore similar between different sites within the London area, even though this cannot be directly verified from the measurements. We thus expect that both the modelled and measured gradients between the urban and the reference sites bear a

clear signature of the anthropogenic emissions from the London area.

The largest hourly ΔCO_2 are observed on the HAC–DET gradient with a mean ($\pm$SD) of 8.2 ± 5.3 ppm. The hourly POP–DET gradients have a mean ($\pm$SD) of 5.6 ± 4.6 ppm. These are much larger than the gradients observed by Rigby et al. (2008) between an 87 m tower in central London at less than 11 km from Hackney and Poplar and a rural location at less than 15 km from Teddington.

The bias, SD and consequently RMS of the model–data discrepancies between modelled and measured gradients of both CO_2 and CH_4 (Table 2) are much reduced compared with the same metrics at individual urban sites (Table 1). The RMS of the model–data discrepancies is roughly halved for ΔCO_2 compared with CO_2 at a single urban site (from 9.0 or 11.7 ppm for the urban sites to 3.6–6.3 ppm for the gradients depending on the corresponding pairs of sites). There is also a small improvement in correlation between observed and modelled ΔCO_2 compared with correlation between observed and modelled CO_2 at individual urban sites (from between 0.02 and 0.13 to between 0.20 and 0.35), but model–data correlations for ΔCH_4 are reduced compared with those for CH_4 at the individual urban sites (from between 0.42 and 0.58 to between 0.20 and 0.30).

The measurements at each site are affected by a constant calibration bias (see Sect. 2.3); therefore, the decrease in model–data biases after the gradient computation partially comes from the cancellation of this systematic error. However, this systematic error (typically ± 1 ppm and ± 5 ppb for CO_2 and CH_4 respectively; Table 1) is much smaller than the difference between the model–data biases when considering the analysis of mole fractions at individual sites (Table 1) and those when considering gradients between these sites (Table 2). Furthermore, the random measurement error should be larger for gradients than at individual sites (since the SD of the measurement error for the difference between two data at individual sites is the RSS of the SD of the independent measurement errors for these data). Therefore, the main driver of the strong decrease in model–data discrepancies when analysing gradients instead of mole fractions at individual sites should be the strong reduction of the large scale errors from the boundary conditions and remote fluxes.

The random component of the measurement errors should be uncorrelated between different sites, and thus the SD of the gradient measurement error should be $\sqrt{2}$ times the SD of the measurement error at individual sites. Therefore, the gradient measurement error should remain much smaller (typically equal to 0.4 ppm and 11 ppb for CO_2 and CH_4 respectively) than the gradient model–data discrepancies (Table 2). The gradient model–data discrepancies should thus mainly be related to model (transport and representation) errors and errors in the estimate of fluxes in the London area, unless a significant influence of the remote fluxes remains in the measured gradients even though this section has shown that such an influence is negligible in the modelled gradients.
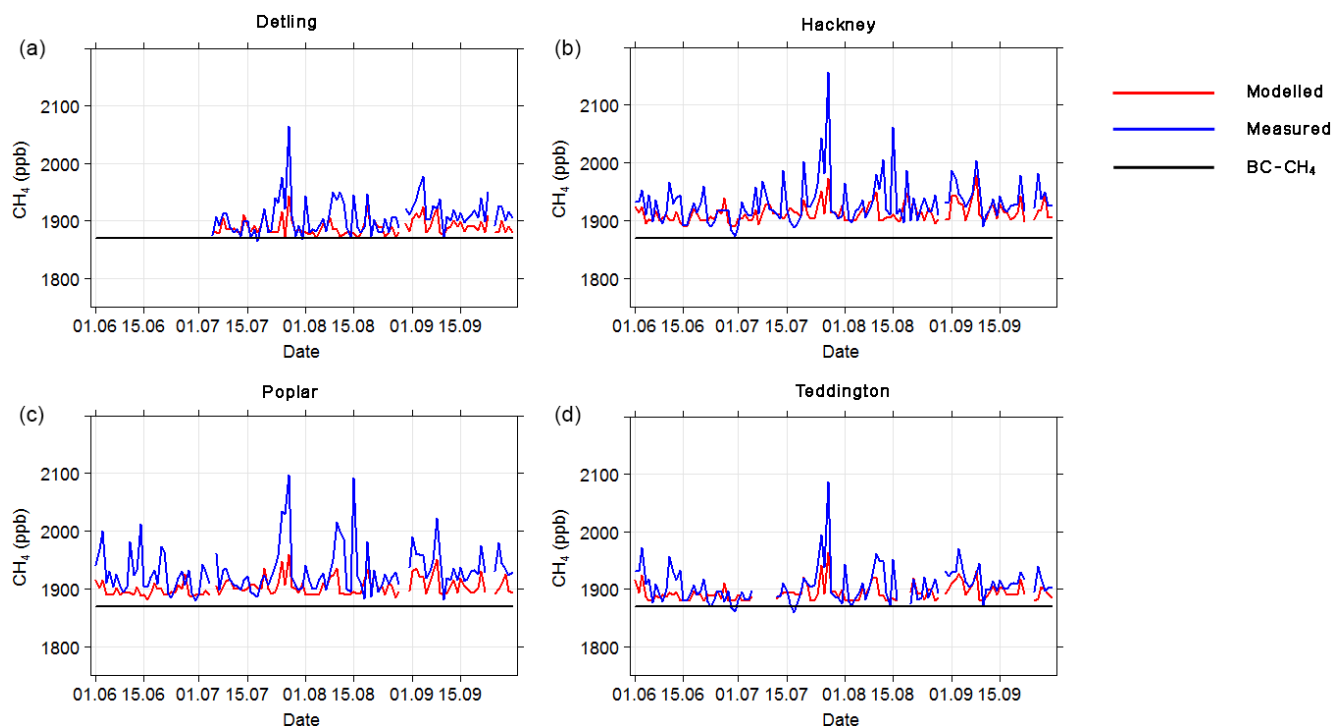
Figure 5. Time series of averages for the afternoon period (12:00 to 17:00 UTC) each day of measured CH_4 mole fractions (blue), modelled CH_4 mole fractions (red) and the constant signature of the modelled CH_4 boundary conditions (BC-CH_4, black) at **(a)** Detling, **(b)** Hackney, **(c)** Poplar and **(d)** Teddington.

Table 2. Summary of systematic and random errors of hourly measured gradients (see Sect. 3.5, the standard deviation of the measurement error for gradients is computed as $\sqrt{2}$ times the value of Table 1, assuming null correlation of this error between different sites) and of the hourly gradient model–data discrepancies using data between 12:00 and 17:00 UTC during July to September 2012. Values are given for ΔCO_2 (ΔCH_4 in brackets) in parts per million (ppm) and parts per billion (ppb) for CH_4. The two last columns present discrepancies for afternoon gradients to Teddington wherein Heathrow measured wind direction places Teddington upwind of each urban site (for angles between the wind direction and the direction between Teddington and a given urban site smaller than 20°, see Sect. 3.6). SD denotes standard deviation; RMS denotes root mean square.

	Gradient measurement error	All afternoon discrepancies				Teddington upwind discrepancies only	
		HAC–DET	POP–DET	HAC–TED	POP–TED	HAC–TED	POP–TED
Bias	SD of bias: 0.0 (0)	−3.8 (−2.6)	−0.2 (−9.7)	−2.9 (−7.1)	0.6 (−16.1)	−1.4 (−3.5)	1.7 (−10.8)
SD	0.4 (11)	5.1 (34.4)	4.4 (36.6)	4.2 (28.3)	3.6 (32.2)	2.9 (14.5)	3.4 (11.0)
RMS	–	6.3 (34.4)	5.1 (29.2)	4.4 (37.8)	3.6 (36.0)	3.2 (14.8)	3.7 (15.3)

3.6 CO_2 and CH_4 gradients with wind direction filtering

Figure 6 shows that the fit between the modelled ΔCO_2 and $\Delta FF-CO_2$ is better for gradients to Teddington than to Detling. Potential explanations could be that Teddington is far closer to London's centre than Detling (Fig. 1), and that Teddington is more frequently upwind of the city than Detling. The signature of fluxes outside the urban area can be assumed to be more homogeneous along the wind direction than over the whole urban area (Bréon et al., 2015;

Staufer et al., 2016), in particular for the measurements (for the model, the boundary conditions and fluxes outside London are prescribed with relatively coarse resolution products, see Sect. 2.4; so this signature is homogeneous over larger spatial scales in the model than in the measurements). Bréon et al. (2015) decreased the signature of the fluxes outside the Paris urban area by considering gradients between two sites along the wind direction rather than by considering all gradients irrespective of the wind condition. Applying this general concept to our study, we expect the gradients to Teddington to be representative of the London urban emissions more
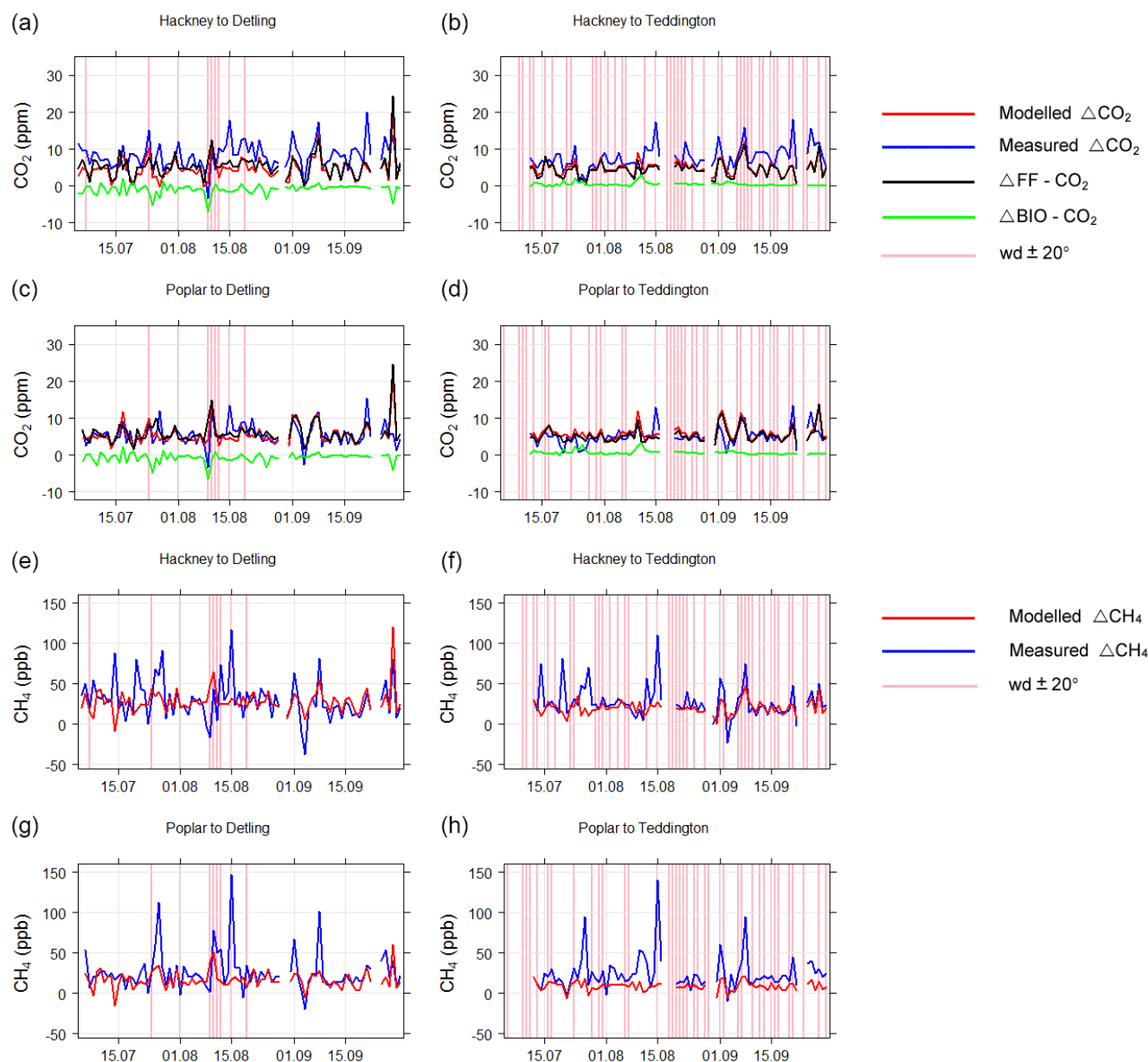
Figure 6. Time series of averages for the afternoon period (12:00 to 17:00 UTC) each day of measured ΔCO_2 (blue), modelled ΔCO_2 (red), modelled signature of the fossil fuel CO_2 emissions (ΔFF-CO_2) (black) and modelled signature of the CO_2 NEE (ΔBIO-CO_2) (green) between **(a)** Hackney and Detling, **(b)** Hackney and Teddington, **(c)** Poplar and Detling and **(d)** Poplar and Teddington. Time series of averages for the afternoon period (12:00 to 17:00 UTC) of measured (blue) or modelled (red) ΔCH_4 between **(e)** Hackney and Detling, **(f)** Hackney and Teddington, **(g)** Poplar and Detling, and **(h)** Poplar and Teddington. Vertical pink lines indicate days during which at least one hourly afternoon wind direction is within a $\pm 20°$ range around the direct line from the reference site to the urban site according to the wind measurements at Heathrow (if the reference site is Teddington) or East Malling (if the reference site is Detling).

often than the gradients to Detling. Measured gradients calculated without considering the wind direction, particularly gradients to Detling, could retain a significant influence of the boundary conditions and fluxes outside the London area (even though this does not occur in the model). In extreme cases, the signature of remote fluxes can be far lower at the urban sites than at Detling (e.g. if Detling, unlike the urban

sites, sees anthropogenic emissions from the continent) so that the signature of the anthropogenic emissions at the urban sites could not compensate for it; this would explain why the measured gradients sometimes reach negative values (e.g. -20.9 ppm for CO_2 on 9 September, while the wind blows from the south-south-west) even though they were computed to isolate the signature of the London emissions (Fig. 6).

Therefore, to reduce the influence of remote fluxes and increase the signature of the London urban emission when analysing both the measured and simulated gradients, we next select gradients for hours in which the corresponding reference site is upwind of the corresponding urban site. In practice, we select the hourly gradient between an urban site and the reference site when the wind direction measured at Heathrow (if the reference site is Teddington) or East Malling (if the reference site is Detling) is within a $\pm 20°$ range around the direction from the reference site to the urban site (which corresponds to the pink shading in Fig. 6). The selected gradients correspond to 22 % (101 over 452) of the available HAC–TED afternoon gradients and 22 % (93 over 431) of the POP–TED available afternoon gradients for either CO_2 or CH_4. There are only 17 hourly (CO_2 or CH_4) gradients to Detling (3 % of all available afternoon gradients to Detling) recorded wherein Detling was positioned upwind of the urban sites. Because of this low number of selected observations, gradients to Detling are ignored in the remainder of the analyses.

The statistics of the model–data discrepancies for gradients to Teddington when this site is upwind the urban sites are presented in Table 2. Filtering for wind direction reduced the negative bias and the RMS of discrepancies for ΔCO_2 HAC–TED gradients, but slightly increased the RMS of discrepancies and increased the positive bias on the ΔCO_2 POP–TED gradient relative to the statistics on the discrepancies without wind filtering. The resulting SD of the discrepancies has values (approximately 2.5–3.5 ppm) that correspond to the typical observation and model transport errors identified by other inverse modelling studies; for example, Bréon et al. (2015) diagnose a 3 ppm SD of the observation error for gradients in the Paris area. However, the bias in ΔCO_2 for both HAC–TED and POP–TED after wind filtering is within the range of 1 to 2 ppm, which remains relatively high compared with the average of these gradients both in the model and in the measurements. There is an underestimation of ΔCO_2 at Hackney and an overestimation of ΔCO_2 at Poplar. Regarding ΔCH_4, all the statistics of the model–data discrepancies after wind filtering are improved substantially, resulting in the RMS discrepancies being roughly halved (from ~ 37 to ~ 15 ppb) when comparing the statistics with and without wind filtering.

To increase the number of selected gradients and thus the robustness of the statistics, we next conduct a test wherein the constraint on the wind direction is relaxed to $\pm 40°$ around the direction from the suburban to the urban site. The resulting bias and RMS of model–data discrepancies for ΔCO_2 are very similar for HAC–TED to those with a range of $\pm 20°$ around the direction from the suburban to the urban site (with bias of -1.8 ppm and RMS of the discrepancies of 3.4 ppm). However, the $\pm 40°$ wind direction improves the statistics at Poplar (with bias of 0.9 ppm and RMS of model–data discrepancies of 3.1 ppm). While this option yields better results in general, it diverges from the principle of monitoring

the gradients of concentration along the transport direction only.

Since local sources have been identified as a potential major source of model–data discrepancies, a further analysis of the gradients when the wind direction is within a $\pm 20°$ range around the direction from the suburban to the urban site is conducted by selecting only gradients to Teddington when both the hourly mean wind speed measured at Heathrow and modelled at Teddington are above $3 \, m \, s^{-1}$. Such a threshold is assumed to decrease the influence of local sources on the variations in the GHG mole fractions (Bréon et al., 2015). However, the sensitivity to this selection is relatively weak and it only slightly improves the results for ΔCO_2 and ΔCH_4 for HAC–TED (i.e. decreases the RMS discrepancies by 0.3 ppm for ΔCO_2 and 2.1 ppb for ΔCH_4) and ΔCH_4 for POP–TED (i.e. decreases the RMS discrepancies by 0.4 ppb) and slightly increases the discrepancies for ΔCO_2 for POP–TED (i.e. increases their RMS by 0.2 ppm), while further decreasing the number of observations (to 82 POP–TED gradients and 87 HAC–TED gradients for either CO_2 or CH_4) and thus reducing the robustness of the statistics.

3.7 Estimation of the fossil fuel component of the CO_2 mole fractions

While the signature of the fossil fuel emissions dominates and the contribution of the natural fluxes is weak in the modelled gradient between urban and suburban CO_2, especially when considering POP–TED and HAC–TED gradients filtered according to the wind direction (Sect. 3.6 and Fig. 6b and d), the contribution of the natural fluxes can be significant even when applying the wind direction filtering for HAC–DET or POP–DET CO_2 gradients (Fig. 6a and c). Furthermore, the CTESSEL model used to simulate the CO_2 NEE does not correctly represent the NEE in the London area (see Sect. 2.4), while the natural fluxes within urban areas can be significant compared with the anthropogenic emissions (Nordbo et al., 2012). These points, the discussions in Sect. 3.6, and the residual discrepancies when comparing measured and modelled gradients question the validity of the assumption that the signature of the natural fluxes is not significant compared with that of the fossil fuel emissions in the measured gradient with or without wind direction filtering.

In this section we thus attempt to improve the focus on the signature of the urban emissions by deriving a CO_2 fossil fuel component from both the modelled and the measured gradients. While the model directly provides the fossil fuel CO_2 gradient ($\Delta FF\text{-}CO_2$) values, we use an empirical method based on the continuous CO measurements to extract an observation-based estimate of $\Delta FF\text{-}CO_2$ between the measurement sites, since CO and CO_2 are co-emitted when fossil fuels are burnt. We focus the analysis on HAC–TED and POP–TED when Teddington is located upwind of the urban sites (with a $\pm 20°$ margin for the selection of the corre-

sponding wind direction), given that such a choice increases the consistency between the model and the data (Sect. 3.6).

The ratio of CO to FF-CO_2 (henceforth R_{CO/CO_2}) varies depending on the different type of sources (e.g. traffic, industry) whose relative influence at the measurement sites can vary in time due to changing traffic and meteorological conditions. However, we assume that these relative influences on HAC–TED and POP–TED gradients are constant in time during the afternoon, when Teddington is upwind of the urban sites. We also assume that CO acts as a conservative tracer and does not interact with the surrounding environment during its transport throughout the London urban area (Gamnitzer et al., 2006). Consequently, we assume that R_{CO/CO_2} resulting from the combination of all sources is constant for gradients between two given sites. Using CO gradients and this ratio, one can derive the observation-based ΔFF-CO_2 using the following equation (Eq. 1):

$$\Delta FF\text{-}CO_2 = \frac{CO_{urb} - CO_{suburb}}{R_{CO/CO_2}}, \tag{1}$$

where CO_{urb} is the observed CO mole fractions at the urban site and CO_{suburb} is the observed CO mole fractions at the suburban Teddington site.

We can assume a traffic-dominated value of R_{CO/CO_2} during summer as we can anticipate lower energy consumption due to natural gas burning in the surrounding area (Vogel et al., 2010). Examination of the diurnal cycle of CO at the urban sites revealed the typical traffic-based variability of increased mole fractions in the early morning and late afternoon and larger CO mole fractions during the day than overnight (Sect. 3.2, Fig. 3b). A value of 0.011 is given to R_{CO/CO_2} based on the literature that has evaluated traffic dominated values of R_{CO/CO_2} in urban areas (in Western areas of the world) using the ^{14}C isotope (Wunch et al., 2009; Vogel et al., 2010; Newman et al., 2013). We further assume that the errors in observation-based ΔFF-CO_2 are smaller than the model or actual ΔFF-CO_2 variations.

Modelled ΔFF-CO_2 is on average slightly larger than observation-based ΔFF-CO_2 on the HAC–TED gradient (observed-based mean ΔFF-$CO_2 \pm$ SD of 6.2 ± 2.3 ppm and modelled mean ΔFF-$CO_2 \pm$ SD of 5.8 ± 3.8 ppm). On the POP–TED gradient, observation-based ΔFF-CO_2 is considerably lower than the modelled ΔFF-CO_2 (observation-based mean ΔFF-$CO_2 \pm$ SD of 3.5 ± 1.0 ppm and modelled mean ΔFF-$CO_2 \pm$ SD of 6.3 ± 2.9 ppm). Statistical comparisons between modelled and observation-based ΔFF-CO_2 mole fractions are given in Table 3. Compared with ΔCO_2 (Table 2), we see a very strong reduction in bias and RMS on the HAC–TED gradient when considering the fossil fuel component only. However, the POP–TED gradients model–data bias is significantly increased when comparing results for ΔFF-CO_2 to those for ΔCO_2 (Tables 2 and 3).

Table 3. Statistics of the hourly difference between modelled and observationally based fossil fuel CO_2 gradients (ΔFF-CO_2) in parts per million (ppm) for HAC–TED and POP–TED during the afternoon periods (12:00 to 17:00 UTC) between July and September, when Heathrow measured wind direction places Teddington upwind of each urban site (for angles between the wind direction and the direction between Teddington and a given urban site smaller than 20°, see Sect. 3.6). RMS denotes root mean square.

Error type	HAC–TED	POP–TED
Bias	−0.4	2.8
RMS	2.5	3.6

4 Concluding remarks

4.1 Summary and discussions

In this study we compared observed CO_2 and CH_4 mole fractions from four near-ground measurement sites in and around London to the simulations from a mesoscale transport model driven by temporally and spatially varying emissions estimates. We aimed to determine whether these near-ground sites would be amenable to the atmospheric inversion of the London city-scale emissions using such an atmospheric transport model. The measurements and model simulation applied to the period June–September 2012. Given the initial diagnostic of very large model–data discrepancies at the different measurement sites, this study attempted to remove or characterise the influence of some of the underlying sources of uncertainty and to isolate, in both the model and the measurements, the signal that corresponds to the London anthropogenic emissions, which would be targeted by the inversion.

Focusing the analysis on afternoon data limited the impact of the model's inability to correctly predict the transitions of the mixing layer depth in morning and evening. This problem was acknowledged in other GHG transport studies (Denning et al., 1999; Geels et al., 2007; Lac et al., 2013). It is possible that this is exacerbated here because of the London urban heat island, which is significant overnight (Barlow et al., 2014; Bohnenstengel et al., 2015), while the model meteorological forcing did not include an urban parameterisation of the heat fluxes.

Focusing the analysis on gradients between the urban sites and the reference sites, especially when selecting them for periods when the suburban reference site was upwind of the urban sites, strongly reduced the impact of errors from the boundary conditions and fluxes outside of the London area in the modelling configuration. Since these boundary conditions and remote fluxes were shown to strongly drive the time variations in the mole fractions in the London area, this focus yielded a relatively low time-varying component of the model–data discrepancies. According to the model, this gradient computation also allowed isolating the signature of

the London anthropogenic emissions from that of the natural fluxes in the area. The very good fit between the modelled fossil fuel CO_2 gradient between Hackney and Teddington (when Teddington is upwind of Hackney) and the CO measurement based estimate of this gradient (even though this estimate relied on crude assumptions regarding the correlation between CO and fossil fuel CO_2) could further support the assumption that the urban to suburban along-wind gradient bears a very strong signature of the London emissions that is consistent between the model and the measurements.

However, there are large biases between the modelled fossil fuel CO_2 gradient between Poplar and Teddington (when Teddington is upwind of Poplar) and the CO measurement-based estimate of this gradient, and between the modelled and measured CO_2 gradients between the urban and reference sites (filtering or not by the wind direction so that the reference site is upwind of the urban site). These biases could be related to biases in the estimate of anthropogenic emissions in the model. However, there is a substantial difference between the measured gradients from Hackney to Teddington and those from Poplar to Teddington, while the model predicts similar gradients when considering either urban site,when considering either the average or the daily variations in the afternoon gradients (Fig. 6b and d). In particular, this results in model–data biases with opposite signs depending on the urban site considered. This indicates that such biases and much of the variations in the gradient model–data discrepancies are likely related to local sources that cannot be represented with the 2 km resolution model rather than to errors in the city-scale estimate of the anthropogenic emissions in the model. Local traffic sources, identified southeast of the Hackney site in Sect. 3.1, should not influence the gradients between Hackney and Teddington when the wind blows from Teddington (on the west) to Hackney (on the east). However, other smaller CO_2 sources are likely to occur nearby to the urban sites.

For CH_4 there is greater similarity between observations and between the model simulations at the two urban sites. This suggests that there are no CH_4 local sources near these sites. This seems reasonable because the major CH_4 point sources in urban environments are mainly related to a limited number of specific waste-processing sites, none of which are located near the measurement sites by the NAEI, or to points of leakage in the gas distribution network, which only represent 20 % of the CH_4 emissions in the London area according to Lowry (2001). This, and the poorer representation of the boundary conditions for CH_4 in the model, can explain why the CH_4 discrepancies were reduced more successfully than the CO_2 discrepancies when switching from the analysis of data at individual sites to the analysis of gradients.

The errors in the meteorological forcing could also contribute to the model–data CO_2 or CH_4 discrepancies even though the analysis did not identify a direct link between them and the model–data wind or mixing layer height discrepancies. The biases between this forcing and measured wind in terms of biases in wind speed ($0.37\,\mathrm{m\,s^{-1}}$, i.e. 7 % of observation mean) and in terms of biases in wind direction (5°, where positive is clockwise) were smaller than reported by other studies (Lac et al., 2013), but could be highly problematic in a urban environment with highly heterogeneous sources in the vicinity of the measurement sites (Bréon et al., 2015). Our analysis also showed that the meteorological forcing used in this study underestimated the mixing layer depth during the afternoon.

Furthermore, we assessed measurement error as a potential source of model–data discrepancies throughout our analyses in this study. Practical constraints for this short measurement campaign did not allow us to design it in such a way that the measurements can be compared with each other or with other measurements within 0.1 ppm, as recommended by WMO for the Northern Hemisphere (WMO & GAW, 2012). The random measurement error at individual sites was smaller than the model–data discrepancies by an order of magnitude and so was considered to be negligible. However, the systematic measurement error is large enough not to be neglected in the raw discrepancies, even though it does not dominate. By definition, the unknown offset in our network vanishes when inter-site gradients are considered, but only because a unique calibration cylinder was used for all sites and for the whole measurement period, which is not a robust solution for larger and longer-lasting local networks. This unknown offset hampers any comparison with other measurement sites in the UK or other places in the world that can therefore not be assimilated in the same inverse modelling system as our London city measurements.

4.2 Conclusion regarding the potential of near-ground measurements for the monitoring of the city-scale emissions

The combined impact of the sources of errors discussed above is such that the amplitude of the model–data discrepancies in the gradients is often as large as that of the measured gradients, in particular for CH_4, which is not optimistic regarding the ability to adjust the estimate of the London urban emissions. McKain et al. (2015) were able to conduct a city-scale assessment of the emissions of Boston, but this relied on the fact that the fugitive CH_4 emissions from the gas distribution network are high in large cities in the US (Phillips et al., 2013). As indicated above, Lowry et al. (2001) showed that such emissions are far lower for a city like London and similar conclusions were raised by recent CH_4 monitoring campaigns in Paris and Rotterdam within the Climate-KIC Carbocount-CITY project (http://www.climate-kic.org/projects/carbon-emissions-from-cities/). In many cities, including London, the major CH_4 emissions do not seem to be spread or significant enough in the urban environment to be monitored using a city-scale atmospheric inversion approach. Monitoring individually (using local-scale inversion techniques; Yver Kwok et al., 2015) the specific CH_4 point

sources dominating the city emissions and which are often located outside the central urban area (landfills, waste water treatment plants and gas compression sites) may thus prove to be more suitable than the city-scale approach in these cities.

For CO_2, the fact that the model–data discrepancies in the gradients, which mainly consist of biases, do not occur at large scale and are likely strongly driven by local sources that cannot be represented with the 2 km resolution transport model raises strong challenges for the inversion of the CO_2 emissions using such a transport model. The location of the measurement sites in the core of the urban area (where the building and traffic is very dense and the topography is made complex by the urban canopy) close to the ground (at less than 15 m a.g.l.), where the sensitivity to local sources is very high, may be responsible for such an issue. Therefore, this study strongly questions the current ability to exploit a GHG network with near-ground urban measurement sites alongside a state-of-the-art atmospheric inversion system with kilometre-scale atmospheric transport models and ignoring the sub-grid-scale variability of such models.

4.3 Perspectives

Bréon et al. (2015) and Staufer et al. (2016) showed that near-ground CO_2 measurements at less than 20 m a.g.l., and located in suburban areas at opposite edges of the urban area, can be used for city-scale CO_2 inversions assimilating cross-city upwind–downwind gradients. Exploiting CO_2 measurements at more than 20 m a.g.l. in the core of the urban area could remain a challenge due to local transport processes and sources, as shown by the analysis of Bréon et al. (2015) for the measurements at the top of the Eiffel Tower in Paris. This challenge may be addressed using networks with different types of urban measurements (e.g. integrated column measurements, Hase et al., 2015), or averaging data from sufficiently dense sampling to obtain information about the spatial scales relevant to the model. Several conceptual improvements of the inversion methodology could also support the exploitation of urban measurements and to determine where, under which conditions and/or how the large-scale signal can be filtered from the measurements so that it could be well represented by the kilometre-scale models. This would require the analysis of the representativity of potential location of the urban measurement sites and of the CO_2 atmospheric variability at very high resolution using, for example, local high-resolution model simulations, mobile measurements, or a very dense array of measurements in a small area. All these measurements and modelling concepts remain to be deployed and tested, but this still leaves some potential for the exploitation of near-ground urban measurements within city-scale inversion frameworks.

Even though this study mainly highlighted the challenges of using near-ground urban measurements, it still strengthened the confidence in specific inversion techniques. The as-

simulation of measurement gradients along the wind direction instead of individual measurements is increasingly used for city-scale activities. However, it is barely used for larger-scale inversion activities. Alternative approaches are used to limit the impact of the uncertainties in the model boundary conditions, such as controlling the signature of these conditions at the different measurements site by the inversion (Lauvaux et al., 2012; Henne et al., 2016). The improvement brought by the gradient analysis and the issues encountered with urban measurement strongly supports the potential of this "gradient approach" and encourages the design of city networks where most stations are located at the edge of the urban area rather than spread evenly in the core of this area. Finally, the improvement of the model–data statistics obtained with a simple approach for deriving observation-based fossil fuel CO_2 gradients from CO gradients demonstrates the need for accurate partitioning of the natural and anthropogenic atmospheric signals even in a city such as London. This increases confidence in the idea that the joint assimilation of CO and CO_2 data could strengthen the potential of the inversion for monitoring the anthropogenic emissions, even though some recent studies highlight the challenge for deriving precise estimates of the (variable) CO / CO_2 anthropogenic emission ratio (Ammoura et al., 2014).

Data availability

The UK Meteorological Office MIDAS data set is available on request from British Atmospheric Data Centre (BADC) archive (http://badc.nerc.ac.uk).

References

Abushammala, M. F. M., Basri, N. E. A., and Younes, M. K.: Seasonal Variation of Landfill Methane and Carbon Dioxide Emissions in a Tropical Climate, International Journal of Environmental Science and Development, 7, 586–590, 2016.

Agustí-Panareda, A., Massart, S., Chevallier, F., Boussetta, S., Balsamo, G., Beljaars, A., Ciais, P., Deutscher, N. M., Engelen, R., Jones, L., Kivi, R., Paris, J.-D., Peuch, V.-H., Sherlock, V., Vermeulen, A. T., Wennberg, P. O., and Wunch, D.: Forecasting global atmospheric CO_2, Atmos. Chem. Phys., 14, 11959–11983, doi:10.5194/acp-14-11959-2014, 2014.

Ammoura, L., Xueref-Remy, I., Gros, V., Baudic, A., Bonsang, B., Petit, J.-E., Perrussel, O., Bonnaire, N., Sciare, J., and Chevallier, F.: Atmospheric measurements of ratios between CO_2 and co-emitted species from traffic: a tunnel study in the Paris megacity, Atmos. Chem. Phys., 14, 12871–12882, doi:10.5194/acp-14-12871-2014, 2014.

Aulagnier, C., Rayner, P., Ciais, P., Vautard, R., Rivier, L., and Ramonet, M.: Is the recent build-up of atmospheric CO_2 over Europe reproduced by models. Part 2: an overview with the atmospheric mesoscale transport model CHIMERE, Tellus B, 62, 14–25, doi:10.1111/j.1600-0889.2009.00443.x, 2010.

Barlow, J. F., Halios, C. H., Lane, S. E., and Wood, C. R.: Observations of urban boundary layer structure during a strong urban heat island event, Environ. Fluid Mech., 15, 1–26, doi:10.1007/s10652-014-9335-6, 2014.

Bieser, J., Aulinge, A., Matthias, V., Quante, M., and van der Gon, H.: Vertical emission profiles for Europe based on plume rise calculations, Environ. Pollut., 159, 2935–2946, doi:10.1016/j.envpol.2011.04.030, 2011.

Bohnenstengel, S. I., Belcher, S. E., Aiken, A., Allan, J. D., Allen, G., Bacak, A., Bannan, T. J., Barlow, J. F., Beddows, D. C. S., Bloss, W. J., Booth, A. M., Chemel, C., Coceal, O., Di Marco, C. F., Dubey, M. K., Faloon, K. H., Fleming, Z. L., Furger, M., Gietl, J. K., Graves, R. R., Green, D. C., Grimmond, C. S. B., Halios, C. H., Hamilton, J. F., Harrison, R. M., Heal, M. R., Heard, D. E., Helfter, C., Herndon, S. C., Holmes, R. E., Hopkins, J. R., Jones, A. M., Kelly, F. J., Kotthaus, S., Langford, B., Lee, J. D., Leigh, R. J., Lewis, A. C., Lidster, R. T., Lopez-Hilfiker, F. D., McQuaid, J. B., Mohr, C., Monks, P. S., Nemitz, E., Ng, N. L., Percival, C. J., Prévôt, A. S. H., Ricketts, H. M. A., Sokhi, R., Stone, D., Thornton, J. A., Tremper, A. H., Valach, A. C., Visser, S., Whalley, L. K., Williams, L. R., Xu, L., Young, D. E., and Zotter, P.: Meteorology, air quality, and health in London: The ClearfLo project, B. Am. Meteorol. Soc., 96, 779–804, doi:10.1175/BAMS-D-12-00245.1, 2015.

Börjesson, G. and Svensson, B. H.: Seasonal and Diurnal Methane Emissions From a Landfill and Their Regulation By Methane Oxidation, Waste Manage. Res., 15, 33–54, doi:10.1177/0734242x9701500104, 1997.

Boussetta, S., Balsamo, G., Beljaars, A., Panareda, A.-A., Calvet, J.-C., Jacobs, C., van den Hurk, B., Viterbo, P., Lafont, S., Dutra, E., Jarlan, L., Balzarolo, M., Papale, D., and van der Werf, G.: Natural land carbon dioxide exchanges in the ECMWF integrated forecasting system: Implementation and offline validation, J. Geophys. Res.-Atmos., 118, 5923–5946, doi:10.1002/jgrd.50488, 2013.

Bréon, F. M., Broquet, G., Puygrenier, V., Chevallier, F., Xueref-Remy, I., Ramonet, M., Dieudonné, E., Lopez, M., Schmidt, M., Perrussel, O., and Ciais, P.: An attempt at estimating Paris area CO_2 emissions from atmospheric concentration measurements, Atmos. Chem. Phys., 15, 1707–1724, doi:10.5194/acp-15-1707-2015, 2015.

Brewer, P. J., Brown, R. J. C., Miller, M. N., Miñarro, M. D., Murugan, A., Milton, M. J. T., and Rhoderick, G. C.: Preparation and Validation of Fully Synthetic Standard Gas Mixtures with Atmospheric Isotopic Composition for Global CO_2 and CH_4 Monitoring, Anal. Chem., 86, 1887–1893, doi:10.1021/ac403982m, 2014.

Broquet, G., Chevallier, F., Rayner, P., Aulagnier, C., Pison, I., Ramonet, M., Schmidt, M., Vermeulen, A. T., and Ciais, P.: A European summertime CO_2 biogenic flux inversion at mesoscale from continuous in situ mixing ratio measurements, J. Geophys. Res.-Atmos., 116, D23303, doi:10.1029/2011jd016202, 2011.

Bush, T., Tsagatakis, I., Passant, N., Griffin, A., and Pearson, B.: UK Emission Mapping Methodology 2007, Didcot, Oxfordshire, ED48954, 52 pp., 2010.

Ciais, P., Paris, J. D., Marland, G., Peylin, P., Piao, S. L., Levin, I., Pregger, T., Scholz, Y., Friedrich, R., Rivier, L., Houwelling, S., Schulze, E. D., and Team, C. S.: The European carbon balance. Part 1: fossil fuel emissions, Glob. Change Biol., 16, 1395–1408, doi:10.1111/j.1365-2486.2009.02098.x, 2010a.

Ciais, P., Rayner, P., Chevallier, F., Bousquet, P., Logan, M., Peylin, P., and Ramonet, M.: Atmospheric inversions for estimating CO_2 fluxes: methods and perspectives, Climatic Change, 103, 69–92, doi:10.1007/s10584-010-9909-3, 2010b.

Denning, A. S., Holzer, M., Gurney, K. R., Heimann, M., Law, R. M., Rayner, P. J., Fung, I. Y., Fan, S.-M., Taguchi, S., Friedlingstein, P., Balkanski, Y., Taylor, J., Maiss, M., and Levin, I.: Three-dimensional transport and concentration of SF6, Tellus B, 51, 266–297, doi:10.1034/j.1600-0889.1999.00012.x, 1999.

Dragosits, U. and Sutton, M. A.: Modelling and mapping UK emissions of ammonia, methane and nitrous oxide from agriculture, nature, waste disposal and other miscellaneous sources for 2009, http://nora.nerc.ac.uk/14265/ (last access: 29 May 2016), 20, 2011.

Emissions Database for Global Atmospheric Research (EDGAR): http://edgar.jrc.ec.europa.eu/index.php, last access: 13 January 2014.

Font, A., Grimmond, C. S. B., Kotthaus, S., Morgui, J. A., Stockdale, C., O'Connor, E., Priestman, M., and Barratt, B.: Daytime CO_2 urban surface fluxes from airborne measurements, eddy-covariance observations and emissions inventory in Greater London, Environ. Pollut., 196, 98–106, doi:10.1016/j.envpol.2014.10.001, 2015.

Gamnitzer, U., Karstens, U., Kromer, B., Neubert, R. E. M., Meijer, H. A. J., Schroeder, H., and Levin, I.: Carbon monoxide: A quantitative tracer for fossil fuel CO_2?, J. Geophys. Res., 111, D22302, doi:10.1029/2005jd006966, 2006.

World Meteorological Organization (WMO) & Global Atmosphere Watch (GAW): 16th WMO/IAEA Meeting on Carbon Dioxide, Other Greenhouse Gases, and Related Measurement Techniques (GGMT-2011), Wellington, New Zealand, 25–28 October 2011, GAW Report No. 206, available at: http://www.wmo.int/pages/prog/arep/gaw/documents/Final_GAW_206_web.pdf (last access: 29 May 2016), 1–2, 2012.

Geels, C., Gloor, M., Ciais, P., Bousquet, P., Peylin, P., Vermeulen, A. T., Dargaville, R., Aalto, T., Brandt, J., Christensen, J. H., Frohn, L. M., Haszpra, L., Karstens, U., Rödenbeck, C., Ramonet, M., Carboni, G., and Santaguida, R.: Comparing atmospheric transport models for future regional inversions over Europe – Part 1: mapping the atmospheric CO_2 signals, Atmos. Chem. Phys., 7, 3461–3479, doi:10.5194/acp-7-3461-2007, 2007.

Gerbig, C., Körner, S., and Lin, J. C.: Vertical mixing in atmospheric tracer transport models: error characterization and propagation, Atmos. Chem. Phys., 8, 591–602, doi:10.5194/acp-8-591-2008, 2008.

Göckede, M., Michalak, A. M., Vickers, D., Turner, D. P., and Law, B. E.: Atmospheric inverse modeling to constrain regional-scale CO$_2$ budgets at high spatial and temporal resolution, J. Geophys. Res.-Atmos., 115, D15113, doi:10.1029/2009JD012257, 2010.

Hansen, M. C. and Reed, B.: A comparison of the IGBP DISCover and University of Maryland 1 km global land cover products, Int. J. Remote Sens., 21, 1365–1373, doi:10.1080/014311600210218, 2000.

Hase, F., Frey, M., Blumenstock, T., Groß, J., Kiel, M., Kohlhepp, R., Mengistu Tsidu, G., Schäfer, K., Sha, M. K., and Orphal, J.: Application of portable FTIR spectrometers for detecting greenhouse gas emissions of the major city Berlin, Atmos. Meas. Tech., 8, 3059–3068, doi:10.5194/amt-8-3059-2015, 2015.

Helfter, C., Famulari, D., Phillips, G. J., Barlow, J. F., Wood, C. R., Grimmond, C. S. B., and Nemitz, E.: Controls of carbon dioxide concentrations and fluxes above central London, Atmos. Chem. Phys., 11, 1913–1928, doi:10.5194/acp-11-1913-2011, 2011.

Henne, S., Brunner, D., Oney, B., Leuenberger, M., Eugster, W., Bamberger, I., Meinhardt, F., Steinbacher, M., and Emmenegger, L.: Validation of the Swiss methane emission inventory by atmospheric observations and inverse modelling, Atmos. Chem. Phys., 16, 3683–3710, doi:10.5194/acp-16-3683-2016, 2016.

Hernandez-Paniagua, I. Y., Lowry, D., Clemitshaw, K. C., Fisher, R. E., France, J. L., Lanoiselle, M., Ramonet, M., and Nisbet, E. G.: Diurnal, seasonal, and annual trends in atmospheric CO$_2$ at southwest London during 2000–2012: Wind sector analysis and comparison with Mace Head, Ireland, Atmos. Environ., 105, 138–147, doi:10.1016/j.atmosenv.2015.01.021, 2015.

Hogan, R. J., Grant, A. L. M., Illingworth, A. J., Pearson, G. N., and O'Connor, E. J.: Vertical velocity variance and skewness in clear and cloud-topped boundary layers as revealed by Doppler lidar, Q. J. Roy. Meteor. Soc., 135, 635–643, doi:10.1002/qj.413, 2009.

Jeong, S., Zhao, C., Andrews, A. E., Bianco, L., Wilczak, J. M., and Fischer, M. L.: Seasonal variation of CH4 emissions from central California, J. Geophys. Res.-Atmos., 117, D11306, doi:10.1029/2011JD016896, 2012.

Jones, S. D., Le Quéré, C., and Rödenbeck, C.: Auto-correlation characteristics of surface ocean pCO$_2$ and air-sea CO$_2$ fluxes, Global Biogeochem. Cy., 26, GB2042, doi:10.1029/2010GB004017, 2012.

Kort, E. A., Angevine, W. M., Duren, R., and Miller, C. E.: Surface observations for monitoring urban fossil fuel CO$_2$ emissions: minimum site location requirements for the Los Angeles megacity, J. Geophys. Res.-Atmos., 118, 1577–1584, doi:10.1002/jgrd.50135, 2013.

Kotthaus, S. and Grimmond, C. S. B.: Identification of Micro-scale Anthropogenic CO$_2$, heat and moisture sources – Processing eddy covariance fluxes for a dense urban environment, Atmos. Environ., 57, 301–316, doi:10.1016/j.atmosenv.2012.04.024, 2012.

Lac, C., Donnelly, R. P., Masson, V., Pal, S., Riette, S., Donier, S., Queguiner, S., Tanguy, G., Ammoura, L., and Xueref-Remy, I.: CO$_2$ dispersion modelling over Paris region within the CO$_2$-MEGAPARIS project, Atmos. Chem. Phys., 13, 4941–4961, doi:10.5194/acp-13-4941-2013, 2013.

Laurent, O., Guemri, A., Yver Kwok, C. E., Rivier, L., Phillippon, C., and Ramonet, M.: ICOS ATC Metrology Lab: metrological performance assessment of GHG analyzers, 18th WMO/IAEA Meeting on Carbon Dioxide, Other Greenhouse Gases, and Related Measurement Techniques (GGMT-2015), La Jolla, California, 13–17 September 2015.

Lauvaux, T., Schuh, A. E., Uliasz, M., Richardson, S., Miles, N., Andrews, A. E., Sweeney, C., Diaz, L. I., Martins, D., Shepson, P. B., and Davis, K. J.: Constraining the CO$_2$ budget of the corn belt: exploring uncertainties from the assumptions in a mesoscale inverse system, Atmos. Chem. Phys., 12, 337–354, doi:10.5194/acp-12-337-2012, 2012.

Levin, I., Hammer, S., Eichelmann, E., and Vogel, F. R.: Verification of greenhouse gas emission reductions: the prospect of atmospheric monitoring in polluted areas, Philos. T. R. Soc. A, 369, 1906–1924, doi:10.1098/rsta.2010.0249, 2011.

Lowry, D., Holmes, C. W., Rata, N. D., O'Brien, P., and Nisbet, E. G.: London methane emissions: Use of diurnal changes in concentration and δ^{13}C to identify urban sources and verify inventories, J. Geophys. Res., 106, 7427, doi:10.1029/2000jd900601, 2001.

MACC-II: www.copernicus-atmosphere.eu, last access: 1 September 2012.

Masuda, S., Suzuki, S., Sano, I., Li, Y.-Y., and Nishimura, O.: The seasonal variation of emission of greenhouse gases from a full-scale sewage treatment plant, Chemosphere, 140, 167–173, doi:10.1016/j.chemosphere.2014.09.042, 2015.

Masutani, M., Schlatter, T. W., Errico, R. M., Stoffelen, A., Andersson, E., Lahoz, W., Woollen, J. S., Emmitt, G. D., Riishøjgaard, L.-P., and Lord, S. J.: Observing system simulation experiments, in: Data Assimilation: Making Sense of Observations, edited by: Lahoz, W. A., Khattatov, B., and Ménard, R., Springer, Berlin, 647–679, 2010.

McKain, K., Wofsy, S. C., Nehrkorn, T., Eluszkiewicz, J., Ehleringer, J. R., and Stephens, B. B.: Assessment of ground-based atmospheric observations for verification of greenhouse gas emissions from an urban region, P. Natl. Acad. Sci. USA, 109, 8423–8428, doi:10.1073/pnas.1116645109, 2012.

McKain, K. K., Down, A., Raciti, S. M., Budney, J., Hutyra, L. R., Floerchinger, C., Herndon, S. C., Nehrkorn, T., Zahniser, M. S., Jackson, R. B., Phillips, N., and Wofsy, S. C.: Methane emissions from natural gas infrastructure and use in the urban region of Boston, Massachusetts, P. Natl. Acad. Sci. USA, 112, 1941–1946, doi:10.1073/pnas.1416261112, 2015.

Met Office Integrated Data Archive System (MIDAS) Land and Marine Surface Stations Data (1853–current): http://badc.nerc.ac.uk/view/badc.nerc.ac.uk__ATOM__dataent_ukmo-midas (last access: 29 September 2013), 2012.

National Atmospheric Emissions Inventory (NAEI): http://naei.defra.gov.uk/, last access: 12 December 2013.

Nakagawa, F., Tsunogai, U., Komatsu, D. D., Yamada, K., Yoshida, N., Moriizumi, J., Nagamine, K., Iida, T., and Ikebe, Y.: Automobile exhaust as a source of ^{13}C and D-enriched atmospheric methane in urban areas, Org. Geochem., 36, 727–738, doi:10.1016/j.orggeochem.2005.01.003, 2005.

Nehrkorn, T., Henderson, J., Leidner, M., Mountain, M., Eluszkiewicz, J., McKain, K., and Wofsy, S.: WRF Simulations of the Urban Circulation in the Salt Lake City Area for CO$_2$ Modeling, J. Appl. Meteorol. Clim., 52, 323–340, doi:10.1175/JAMC-D-12-061.1, 2013.

Newman, S., Jeong, S., Fischer, M. L., Xu, X., Haman, C. L., Lefer, B., Alvarez, S., Rappenglueck, B., Kort, E. A., Andrews, A. E.,

Peischl, J., Gurney, K. R., Miller, C. E., and Yung, Y. L.: Diurnal tracking of anthropogenic CO_2 emissions in the Los Angeles basin megacity during spring 2010, Atmos. Chem. Phys., 13, 4359–4372, doi:10.5194/acp-13-4359-2013, 2013.

NOAA Mace Head Atmospheric Station Data: http://www.esrl.noaa.gov/gmd/dv/data/?site=MHD (last access: 23 January 2014), 2013.

Nordbo, A., Järvi, L., Haapanala, S., Wood, C. R., and Vesala, T.: Fraction of natural area as main predictor of net CO_2 emissions from cities, Geophys. Res. Lett., 39, L20802, doi:10.1029/2012gl053087, 2012.

O'Shea, S. J., Allen, G., Fleming, Z. L., Bauguitte, S. J. B., Percival, C. J., Gallagher, M. W., Lee, J., Helfter, C., and Nemitz, E.: Area fluxes of carbon dioxide, methane, and carbon monoxide derived from airborne measurements around Greater London: A case study during summer 2012, J. Geophys. Res.-Atmos., 119, 4940–4952, 2014.

Phillips, N. G., Ackley, R., Crosson, E.R., Down, A., Hutyra, L. R., Brondfield, M., Karr, J. D., Zhao, K., and Jackson, R. B.: Mapping urban pipeline leaks: Methane leaks across Boston, Environ. Pollut., 173, 1–4, doi:10.1016/j.envpol.2012.11.003, 2013.

Pregger, T. and Friedrich, R.: Effective pollutant emission heights for atmospheric transport modelling based on real-world information, Environ. Pollut., 157, 552–560, doi:10.1016/j.envpol.2008.09.027, 2009.

Reis, S., Lang, M., and Vieno, M.: Improving the temporal profiles of emission input data for high resolution atmospheric transport modeling-a case study for the UK, 18th Annual International Emission Inventory Conference, Baltimore, USA, 2009.

Rella, C. W., Chen, H., Andrews, A. E., Filges, A., Gerbig, C., Hatakka, J., Karion, A., Miles, N. L., Richardson, S. J., Steinbacher, M., Sweeney, C., Wastine, B., and Zellweger, C.: High accuracy measurements of dry mole fractions of carbon dioxide and methane in humid air, Atmos. Meas. Tech., 6, 837–860, doi:10.5194/amt-6-837-2013, 2013.

Rigby, M., Toumi, R., Fisher, R., Lowry, D., and Nisbet, E. G.: First continuous measurements of CO_2 mixing ratio in central London using a compact diffusion probe, Atmos. Environ., 42, 8943–8953, doi:10.1016/j.atmosenv.2008.06.040, 2008.

Schmidt, H., Derognat, C., Vautard, R., and Beekmann, M.: A comparison of simulated and observed ozone mixing ratios for the summer of 1998 in Western Europe, Atmos. Environ., 35, 6277–6297, doi:10.1016/s1352-2310(01)00451-4, 2001.

Staufer, J., Broquet, G., Bréon, F.-M., Puygrenier, V., Chevallier, F., Xueref-Rémy, I., Dieudonné, E., Lopez, M., Schmidt, M., Ramonet, M., Perrussel, O., Lac, C., Wu, L., and Ciais, P.: A first year-long estimate of the Paris region fossil fuel CO_2 emissions based on atmospheric inversion, Atmos. Chem. Phys. Discuss., doi:10.5194/acp-2016-191, in review, 2016.

Townsend-Small, A., Tyler, S. C., Pataki, D. E., Xu, X., and Christensen, L. E.: Isotopic measurements of atmospheric methane in Los Angeles, California, USA: Influence of "fugitive" fossil fuel emissions, J. Geophys. Res., 117, D07308, doi:10.1029/2011jd016826, 2012.

Turnbull, J. C., Sweeney, C., Karion, A., Newberger, T., Lehman, S. J., Tans, P. P., Davis, K. J., Lauvaux, T., Miles, N. L., Richardson, S. J., Cambaliza, M. O., Shepson, P. B., Gurney, K., Patarasuk, R., and Razlivanov, I.: Toward quantification and source sector identification of fossil fuel CO_2 emissions from an urban area: Results from the INFLUX experiment, J. Geophys. Res.-Atmos., 120, 292–312, doi:10.1002/2014JD022555, 2015.

United Nations: Department of Economic and Social Affairs, Population Division (2013), World Population Prospects: The 2012 Revision, Highlights and Advance Tables, Working Paper No. ESA/P/WP.228, available at: http://esa.un.org/unpd/wpp/publications/Files/WPP2012_HIGHLIGHTS.pdf (last access: 29 May 2016), 2012

Vogel, F. R., Hammer, S., Steinhof, A., Kromer, B., and Levin, I.: Implication of weekly and diurnal ^{14}C calibration on hourly estimates of CO-based fossil fuel CO_2 at a moderately polluted site in southwestern Germany, Tellus B, 62, 512–520, doi:10.1111/j.1600-0889.2010.00477.x, 2010.

Ward, H. C., Kotthaus, S., Grimmond, C. S. B., Bjorkegren, A., Wilkinson, M., Morrison, W. T. J., Evans, J. G., Morison, J. I. L., and Iamarino, M.: Effects of urban density on carbon dioxide exchanges: Observations of dense urban, suburban and woodland areas of southern England, Environ. Pollut., 198, 186–200, doi:10.1016/j.envpol.2014.12.031, 2015.

Wu, L., Broquet, G., Ciais, P., Bellassen, V., Vogel, F., Chevallier, F., Xueref-Remy, I., and Wang, Y.: Atmospheric inversion for cost effective quantification of city CO_2 emissions, Atmos. Chem. Phys. Discuss., 15, 30693–30756, doi:10.5194/acpd-15-30693-2015, 2015.

Wunch, D., Wennberg, P. O., Toon, G. C., Keppel-Aleks, G., and Yavin, Y. G.: Emissions of greenhouse gases from a North American megacity, Geophys. Res. Lett., 36, L15810, doi:10.1029/2009gl039825, 2009.

Yver Kwok, C. E., Müller, D., Caldow, C., Lebègue, B., Mønster, J. G., Rella, C. W., Scheutz, C., Schmidt, M., Ramonet, M., Warneke, T., Broquet, G., and Ciais, P.: Methane emission estimates using chamber and tracer release experiments for a municipal waste water treatment plant, Atmos. Meas. Tech., 8, 2853–2867, doi:10.5194/amt-8-2853-2015, 2015.

Zellweger, C., Steinbacher, M., and Buchmann, B.: Evaluation of new laser spectrometer techniques for in-situ carbon monoxide measurements, Atmos. Meas. Tech., 5, 2555–2567, doi:10.5194/amt-5-2555-2012, 2012.